Aus der Klinik für Orthopädie

(Direktor (komm.) Prof. Dr. med. H. M. Klinger)

im Zentrum Unfallchirurgie und Orthopädie

der Medizinischen Fakultät der Universität Göttingen

The quality of the mechanical properties of laser welded points between commercial pure titanium rings, for creating a net for surgical applications

INAUGURAL – DISSERTATION

zur Erlangung des Doktorgrades

der Medizinischen Fakultät der

Georg-August-Universität zu Göttingen

vorgelegt von

Stelios Ioannou

aus

Nikosia – Zypern

Göttingen 2015

Dekan: Prof. Dr. rer. nat. H. K. Kroemer

I. Berichterstatter: Prof. Dr. med. Wolfgang Schultz
II. Berichterstatter/in: PD Dr. med. Wolfram Hahn
III. Berichterstatter/in:

Tag der mündlichen Prüfung: 14.09.2015

Contents

		Pages
	Abbreviation list	5
CHAPTER I	**Introduction**	6
	1.1 The aim and the contribution of the project in medicine	7
	1.2 Research questions	8
CHAPTER II	**Literature review**	9
	2.1 History of metal alloys for orthopedic and craniofacial medical devices	9
	2.2 Biomaterial requirements	10
	2.3 The spectrum of biomaterials	11
	2.4 Metallic Biomaterials	12
	2.5 The RRM (Reinforced Ring Mesh) made of commercial pure (CP) titanium grade 4 is proposed as a possible biomaterial solution	14
	2.6 Laser	15
	2.6.1 Use of Nd-YAG Laser	15
	2.6.2 Welding procedure on commercial pure (CP) titanium surface	16
	2.7 Tensile testing of materials	16
	2.7.1 Mechanical properties of a device derived from a tensile test	17
CHAPTER III	**Materials and Methods**	20
	3.1 Material description	20
	3.2 Material preparation	21
	3.3 Experimental equipment	22
	3.4 Research protocol	25
CHAPTER IV	**Results**	29
	4.1 Phase A	29
	4.2 Phase B	35
	4.3 Phase C	37
	4.4 Phase D	44
CHAPTER V	**Discussion**	48
	Conclusion	52

Reference list 53

Annex 56

Acknowledgments 69

Abbreviation list

RRM: Reinforced ring mesh

CP: commercial pure

MP: multiphase

Nd-YAG: Neodymium-doped Yttrium Aluminium Garnet

Ti: Titanium

ASTM: American society of testing and materials

Co: Cobalt

Cr: Chromium

Mo: Molybdenum

Al: Aluminium

V: Vanadium

MPa: Megapascal

UTS: Ultimate tensile strength

A: Ampere

ms: millisecond

J: Joule

CHAPTER I

Introduction

Biomaterials seem to be the center of interest for medical surgical procedures in the near future. Biomaterials are used in medicine in several surgical applications such as in orthopedics with hip replacement, knee prosthesis, shoulder prosthesis, stabilization of fragmented bone with plates and in many other applications that restore the damaged body area. Biomaterials are also used in cardiovascular surgery, like the stent application and also for the heart valve replacement. The biomaterials are used in ophthalmology, in dentistry and also in otorhinolaryngology with cochlear implants.

Very important, is the use of biomaterials in orthopedic surgery. In this dissertation a new candidate implant material is introduced, the so-called Reinforced Ring Mesh (RRM). This material makes use of commercially available ring mesh, produced for general safety applications. To most of the readers, ring mesh is known from antique armour: chain mail. The principle of the mesh is the interconnection of rings; a common pattern is the "1-to-4-mesh" where every single ring is connected with four others. This experimental work is the first fundamental experiment to demonstrate the realization of the principal idea and it describes a laser welding process to modify the flexible ring mesh into a rigid strap of interwoven rings. Precise welding of the contact points between these rings is a prerequisite for any clinical application. The welding area quality and the tensile properties of the product are investigated to prove the possible applications of the RRM on the skeletal system. The idea and patent of the RRM comes from the orthopedic department of the university medical hospital Göttingen in Germany by the contribution of Buchhorn G.H., Schultz W. and Wellnitz J: Offenlegungsschrift (Patent number) DE 10 2005 055 432 A1:/ 2008.05.29 "Bauteil aus Geflechtelementen" – "Components made of braided elements" (see Annex).

The RRM implant device, sets as a goal to support and restore structural bone defects such as skull bone tumors, bone gaps after trauma and in general, all bone fractures. The replication of the anatomical bone structures shall allow refixation of bone fragments, support function and provide structures for application of additional functional components. The main goal of RRM is the protection of soft tissues, for example the brain under the restored skull bone, as well as restoration in a pleaseing aesthetic character, which will leave no unwanted postoperative deformities to the patient's bone. The RRM could be applied in craniofacial trauma or in craniosynostotic congenital disorders or some other examples could be the distal humeral fractures, radial head fractures and proximal ulna fractures as well as the fragmented femoral and proximal tibia fractures.

1.1 The aim and the contribution of the project in medicine

The RRM is proposed to be used in disciplines like orthopedic and craniofacial surgery traumas, where in some cases a quarter of the skull is splintered and the use of plates cannot be the best decision to heal the fractured bone. In this case, a mirror image of the rest half of the skull can be taken and an implant made of RRM can be modelled according to the exact dimensions of the skull shape and then can be surgically applied on the fractured half.

Furthermore, this project can contribute also in situations where congenital skull deformities are present. Such occasions are the non-syndromic craniosynostosis, which it takes a percentage of 80-85% among a prevalence of 1:2500 of the different craniosynostotic deformities (Van Veelen-Vincent et al. 2010). The non-syndromic craniosynostosis is associated with a lot of functional problems such as high intracranial pressure, developmental delay and visual disturbances (Van Veelen-Vincent et al. 2010).

In order to follow a procedure and experiments on something new, some problematic reasons and some disadvantages of the already applied medical devices and methods must exist, which guide the scientists to invent something innovative. In this instance, RRM seems to have many more advantages than disadvantages as a new idea. Moreover it also seems to have fewer disadvantages if it is compared with other medical devices that are nowadays applied in orthopedic and craniofacial surgery.

The fields that we are interested in are orthopedic and craniofacial surgery. The use of plates in both disciplines restricts the application of the plate on the fractured bone and according to some studies “rigid plates may evoke stress-forces within the callus during its formation and in the mass of the bone causing ischaemia under the area of the plate” (Lazaridis et al. 1998, p.227). This important disadvantage is overcome with RRM. In orthopedics the implants are formed more or less in the dimensions of the bone but the need for prebending of the plate is essential in order for the implant to be fixed on the bone (Leung 1994). The important reasons for the application of RRM are to overcome the stiffness of the plates, which cannot easily take the shape of the bone, and to apply in some of these situations the formable RRM. The other reason is to achieve a quick osseointegration within the bone gap or the multifragmented fracture due to the micro movements allowed by the mesh. Another benefit of the RRM is the avoidance of postoperative removal of the biomaterial because of its biocompatible character, where this can be profitable for the patient. Furthermore, the RRM with its aesthetic form will leave postoperative no unwanted bone deformities and the difference that could made in contrast to the already applicable titanium mesh is the possibility to be designed and manufactured in a hospital using only the Nd-YAG laser with the necessary welding energy. Moreover, because of its form and formable shape the application of RRM causes less irritation of tendons and muscle tissues, which means minimal inflammation postoperatively.

The contribution of this project is to test the tensile strength of the RRM and thus, to express whether the welded RRM quality is good enough to produce a medical device, which will probably avoid those functional problems and also to its aesthetically pleasing character without the need for removal.

1.2 Research questions

This project sets out to establish the need and a probable future contribution of the RRM in medicine and to perform a number of experiments to evaluate the quality and tensile properties of the welded RRM. For validity purposes, the project will engage aspects concerning the disciplines of physics, chemistry and biomechanics to analyze better and in detail the concept of the study. Particularly these experiments intend to examine the following research questions:

- Is it at all possible to provide a medical device using the welded RRM designed to the bone dimensions?
- Does laser welding process work effectively to provide a stable medical device?
- What is the optimum energy that should be applied on the contact points?
- Do the optimum laser parameters provide reliable mechanical properties results?
- Are there are any significant tensile strength differences between the welded and non-welded specimens?

CHAPTER II

Literature review

2.1 History of metal alloys for orthopedic and craniofacial medical devices

The history of biomaterials and especially the history of metal alloys for orthopedic and craniofacial medical devices are very important for the evolution of new medical devices in these fields of study.

In the late 18^{th} until 19^{th} century they were used various metal devices to fix bone fractures, which were generally unsuccessful as a result of infections. The use of biomaterials became practical in the 1860s, where Dr. J. Lister developed aseptic surgical techniques and he introduced also metal wires to fix even closed fractures since 1870. The first fracture fixation with metal plates in the body had been used in 1886 by the German surgeon H. Hansmann. Another contributor to the use of internal fixation in the fracture treatment, was the Scottish surgeon WA Lane. In 1893 until 1912 W.A. Lane, was the first who developed systems of metal plates and steel screws for internal bone fixation. (Lesić et al. 2012; Park 2000). According to Park (2000) bone plates were used in early 1900s to fix long bone fractures. Many of these early plates broke, because their mechanical design was too thin and had stress corners. Furthermore, the chosen material such as vanadium steel has good mechanical properties. Despite that it corroded rapidly in the body and caused adverse effects on the healing processes. Due to that, they were followed better medical device designs and biomaterials.

Later on, in 1926 stainless steel was applied in orthopaedic implant devices as a corrosion resistant material, but it took not so long for the introduction of another metal alloy the cobalt chrome, which was first used by Drs C.S. Venable and W.G. Stuck. The innovation brought in 1950 the first use of titanium alloy with its extraordinary biocompatible properties (Park 2000). Until then, the most biocompatible metal used for implants was the commercial pure titanium (CP Ti) and titanium alloy (Ti6Al4V). Furthermore, titanium was first discovered in 1791 by the British chemist Reverend William Gregor. Thus, at first titanium was named gregorite. Titanium was at the same time discovered by the German chemist M.H. Klaproth in 1793. He gave it the name titanium according to the Titans of the greek mythology, “the incarnation of natural strength”. Four years later the German chemist realized that the titanium he discovered, was the same element as that of the British chemist William Gregor (WizCom Technologies Ltd 2007).

On the earth crust titanium is the fourth most abundant structural element. Titanium exists only in chemical combinations. In addition, the concentrated sources of titanium in earth crust are the minerals ilmenite, titanomagnetite, rutile, anatase and brookite. (Welsch et al. 2007)

The first titanium craniofacial implant was a mesh used in the Vietnam war in 1968 (Costantino et al. 2009). Since then the use of Titanium as a biomaterial is considered the most biocompatible biomaterial and the titanium plates and also titanium mesh are in use today.

2.2 Biomaterial requirements

First of all the terms *"biomaterial"* and *"biocompatibility"* should be defined. The definition of these two words is important as they are the core for the production of any medical device. The definition of the word *"biomaterials"* is:

> "*A biomaterial is a nonviable material used in a medical device, intended to interact with biological systems*" (Williams 1987)

The word "*biocompatibility*" is defined as follows:

> "*Biocompatibility is the ability of a material to perform with an appropriate host response in a specific application"* (Williams 1987)

By taking into consideration the definitions of those two words it is much easier to understand the use of medical devices and the approach of scientists to conceive suitable implants.

New biomaterials, need for their development an interdisciplinary effort, the cooperation of scientists from different disciplines like material scientists, engineers, biomedical engineers, pathologists and clinicians to raise the potential of researching, developing biomaterials already in use or even to invent new medical devices which will contribute to a new era in medicine.

There are a variety of properties that are required for the medical application of the biomaterials. Physical properties that are required are tensile strength, elastic modulus (*Young's Module*) elongation, yield strength and hardness (Kumar, Patel 2013).

Furthermore, the physical properties are not the only requirement for the medical devices. The medical implants should fulfill some important essential aspects for human health and ethical considerations. This dissertation sets as a goal to examine the tensile properties of the material with which through experiments will illustrate the quality of the welded material, whereas the other subjects are part of further studies.

2.3 The spectrum of biomaterials

The spectrum of biomaterials used in medicine is divided into four major categories. There are, polymers, ceramics, metals and natural materials. Obeying the manifold requirements scientists tend to select biomaterials for special applications according to their optimum material property. A differentiation has to be made e. g. between short- and long-term implants, stable or resorbable materials, high or low mechanical demand, articulation or firm implant – tissue bonds and others. It is accepted practice to compose modular devices where special materials requirements need to be fulfilled. Thus, compromises become necessary to select special material qualities for the best performance. Despite the focus of this dissertation on metallic biomaterials, it is necessary to understand the principles of each category and how it contributes in medicine with the best possible results on medical devices.

Polymers denote the largest category of biomaterials. They are derived either from natural sources or synthetic organic processes. Polymers, have the advantage of being stable and at the same time flexible, thus they are suitable for low friction articulating surfaces like joint replacement. Polymers are used in medicine as intraocular lenses, sutures and hernia repair, catheters, vascular grafts, heart valves, tubing and blood storage bags, breast implants, finger joints, ear, chin and nose reconstruction and also for insulation for pacemaker leads. These medical applications are some of the wide spectrum of polymers applied in medicine and contribute in medicine at its maximum (Cooper et al. 2004).

Ceramics are solid biomaterials that are made of polycrystalline compounds composite usually from inorganic elements including either metallic oxides or non-metallic oxides and also ionic salts. Soluble, (bone substitute material (hydroxyapatite, calciumphosphate ceramics)) / insoluble ceramics (Aluminium oxide (ISO 6474), Y-stabilized zirconium oxide (ISO 13356)) and ceramic composites (ISO 6474-2). Their hardness and wear resistance bring bioceramics in a position of a broad use in medicine. Ceramics are used in applications such as femoral heads, bone screws and bone plates. Due to their characteristics they perform a structural-supporting role (Billotte 2000).

Metal alloys are also one of the most used materials of medical devices. The widely used metals are stainless steel (e.g. 316L grade 2), cobalt-based alloys, and titanium-based alloys. Due to their molecules metallic bonding, metal alloys have the ideal properties to be used in the body to stabilize bone fractures and thus, to withstand heavy loads and to help in this way in the daily life of the people (e. g. walking, chewing etc.) In their majority metals are used in orthopedics and craniofacial surgery, with the use of femoral stems, bone plates and screws. They are also used in cardiovascular surgery as stents and pacemaker sheathings / encapsulations. (Brunski 2004)

2.4 Metallic Biomaterials

According to section 2.3 the metallic biomaterials play an important role in the medical prosthetics. From the very old days, the scientists used to be in a persistent search for metals that will be biocompatible. The most commonly used metallic biomaterials are stainless steel 316L grade 2, cobalt-based alloys and commercial pure (CP) titanium and titanium based alloys.

Stainless steel is provided in different types, which enable their use as medical implants. Despite that, the most commonly used stainless steel type for short-term applications is 316L (ASTM F138, F139, ISO 5832-1) grade 2. The chemical composition of this type is low of carbon. The advantage of these low amounts of carbon is that it reduces the possibility of corrosion *in vivo.* Stainless steel 316L is composite predominantly from iron (60-65%) with significant alloy additions of chromium (17-20%) and nickel (12-14%), furthermore other elements in low amounts, but with a significant role in the chemical properties of the material are nitrogen, manganese, molybdenum, phosphorus, silicon and sulfur. The use of chromium in the material performs a key role for the corrosion resistant property of the stainless steel by forming a strongly adherent surface oxide (Cr_2O_3) (passivation). In addition to that chromium tends to stabilize the ferritic phase of iron. Moreover, silicon and molybdenum work as ferritic stabilizers like chromium. For long-term applications (e. g. femoral endosteal stems) high nitrogen alloys with minimal content of nickel (1 – 2 %) (ASTM F1586, ISO 5832-9) are preferred. (Brunski 2004)

Cobalt is a well-known element in the manufacture of medical devices and aerospace industries. Cobalt based alloys include the “grandfather material” Hayness-Stellite 21 and 25 (ASTM F75, ISO 5832-4 and F90, ISO 5832-5 respectively), and modern cast and forged Co-Cr-Mo alloys (ASTM F799). The frequency of multiphase (MP) alloy MP35N (ASTM F562, ISO 5832-6) applications was reduced as the high content of nickel (35 vol%) raised some concern (Brunski 2004). The Co-based alloys are selectively manufactured to provide various physical and mechanical properties required for the different medical applications. The special features of this material, such as the corrosion resistance, high stiffness and the high wear resistance made it extraordinary in high demand long-term applications. Thus, they are used for a variety of dental, orthopedic, neurological, and cardiovascular applications. (Disegi et al. 1999)

Interesting in the physical, mechanical and chemical properties which make the titanium and its alloys a favorite material for medical devices are the low density (60% less than that of steel), it transfers heat well and is nonmagnetic and it has a high melting point (1650°C), higher than steel (WizCom Technologies Ltd 2007). Titanium, is at the time the best biocompatible metal element.

Titanium exists in two main crystal structures, either pure (with some additional elements for stabilization) or alloy form. In one, the atoms are arranged in a close-packed hexagonal array, the so-called alpha-phase and in the other crystal structure the atoms are arranged in a body-centered cubic array, which is called the beta-phase. Furthermore, titanium is divided into two more types apart from the a-phase and b-phase. It is divided into the near alpha and a+b phase.

Alpha and near alpha alloys demonstrate the best corrosion resistance and weldability, whereas the a+b alloys provide an excellent combination of strength and ductility. In addition to that they are stronger than alpha or beta alloys. Well worth to mention is the ability of an alpha alloy in the presence of certain additional elements and under heat treatment (about 880°C) to be developed into an a+b alloy. On the other hand beta alloys are metastable; this means that they tend to achieve a balance in their structure (Donachie 2000).

For the experimental project, is important to be aware that the CP Titanium Grade 4 (alpha-phase) has a very good weldability (Donachie 2000).

Commercial pure titanium is an alpha phase alloy and due to its properties is assumed to be the best material that can be used for the production of the RRM medical device. Representative of alpha phase is CP-Ti (unalloyed Ti) whereas Ti6Al4V is most often used among the alpha-beta alloys for clinical applications in need of high flexural strength. (Donachie 2000)

2.5 The RRM (Reinforced Ring Mesh) made of commercial pure (CP) titanium grade 4 is proposed as a possible biomaterial solution

CP titanium grade 4 is the best choice of a material to be used for this experimental project. It is obvious that the commercial pure titanium is an alpha phase material with the best corrosion resistance and the best weldability. (Donachie 2000) The goal of the project is to weld the contact points of rings with precision and with no alteration (impairment) of the mechanical properties, whereas the good weldability and corrosion resistance of CP titanium is expected to lead to very good results.

Furthermore, the grade 4 titanium has the best tensile strength 550 MPa among the unalloyed materials, whereas grade 1 has 240 MPa, grade 2 340 MPa, grade 3 450 MPa, grade 7 340 MPa and grade 11 240 MPa (Donachie 2000). On the other hand very important for the project is that this material has minimal additives of elements which means that in high temperatures reaching the melting point, the welded joint and some area around the welded region is turned physically from alpha phase to the alpha + beta phase. Compared to the basic material this transition in crystalline structure would result in a stronger bonding of the welded region if the laser parameters achieve the best possible results. According to this important information the experiment proceeds to be done with the material CP titanium grade 4.

2.6 Laser

One of the most important technical discoveries of the 20th century was the invention and the development of laser. The abbreviation laser means *Light Amplification by Stimulated Emission of Radiation*. The name laser has a long history, starting from 1900 with the work published by the German scientist Max Plank who provided the idea that light is a form of electromagnetic radiation. This perception was the source of understanding how later laser works. Seventeen years later, in 1917 Albert Einstein described the theory of stimulated emission, which moves a step forward in the explanation of how a laser could work. At the time these two scientists could not imagine their contribution in science that the invention of laser depended on their theories. Around 1950 scientists like Charles Townes, Arthur Skawlow, Joseph Weber, Alexander Prokhorov and Nikolai Basov were working independently from each other, towards the creation of the so-called MASER. In abbreviation, MASER means *Microwave Amplification by the Stimulated Emission of Radiation*. MASER works with the same technology like laser with the difference that it emits instead of light radiation, a microwave radiation. In 1960 Theodore Maiman invented the ruby laser, but despite that, there is a misunderstanding of who really is the first inventor of the LASER. Gordon Gould the doctoral student of Charles Townes at the Columbia University was actually the first man who named the light emission LASER (Townes 1999). After Theodore Maiman, the manner of laser development was raised incredibly from many scientists. Nowadays, we use different types of lasers for a variety of applications, from welding and building heavy industry like airplanes, cars, ships etc. and to tiny welding procedures constructing pacemakers and welding titanium used in dentistry. What makes laser to be extraordinary equipment are the qualities intensity, directionality, coherence and monochromaticity (Hecht 1998). Laser is nowadays the equipment that can be used almost everywhere either for welding or cutting due to its properties and precision on the working piece.

2.6.1 Use of Nd-YAG Laser

As it is mentioned in 2.6 there are nowadays a lot of different types of lasers which can be used each one for different reasons. There are mainly three types of solid state lasers: the ruby, neodymium glass, and the neodymium yttrium aluminium garnet (Nd-YAG). Between the three types the neodymium yttrium aluminium garnet is more appropriate for welding procedures, where high quality welding production is required (Dawes 1992). Consequently, for the experimental project of the RRM an Nd-YAG laser is used for the best possible results.

In addition to that, it is important to understand the physics and the function of the Nd-YAG laser. The functional principle is as follows, a pumping source excites the electrons of the medium in the glass container. According to quantum physics the relaxing electrons release the surplus energy named photons. These photons are repeatedly reflected from the mirrors at both edges and are emitted as soon as they achieve a coherent phase as a laser beam passing the partially reflecting mirror at one of the two sides. Nd-YAG lasers work with Neodymium as active laser medium. Reflectors and mirrors enhance the laser beam, Nd YAG lasers emit beams of 1.06 μm wavelength and the laser itself is submerged in a cooling water chamber. (Dawes 1992)

2.6.2 Welding procedure on commercial pure (CP) titanium surface

The laser welding method is divided into two types: (a) the heat conducting welding and (b) the deep penetration welding.

In heat conducting welding method the laser beam energy is absorbed by the two metal components. After conflux of the melts and extinction of the beam, the solidifying melt joins the two metal pieces. This procedure is done for metals around 1.5mm thick. The deep penetration welding is applied for metals with thickness on a scale from some tenths of millimetres to 20mm, in some cases more than 20mm. For the deep penetration welding procedure, the laser beam hits with a certain amount of energy the point of bonding. Melting the contact area of the two metals, the proceeding laser beam displaces the molten material forming a so-called keyhole. The hole behind the beam is filled with the solidifying melt. A plasma cloud of gaseous material surrounds the laser beam (Wolf 2011).

2.7 Tensile testing of materials

The tensile testing of materials is an important step for the selection of a material for a specific purpose, whether this is for the building of an aircraft or for the creation of a medical device like the medical implant of RRM. Mechanical properties derived from a tensile test are used as information in the specification of a material in a standardized composition and manufacturing process to ensure its quality.

Mechanical properties, indicate how the material reacts to forces being applied e.g. in tension. Tensile test is a mechanical test that is performed on a prepared specimen, where it is loaded in a controlled manner while the applied load and elongation of the specimen are measured over some distance. The tensile test can provide to the scientist useful information by determining the Young's modulus, elastic limit, proportional limit, reduction in area, yield point, tensile strength and yield strength. However, the most important outcome is the stress-strain curve, where every material creates its own stress-strain curve.

Furthermore, it is important to know with what equipment the tests are performed. For the performance of a tensile test two types of testing machines are used. The one is the electromechanical machine and the other is the hydraulic machine. The first one, the electromechanical machine has the advantage in contrast to the hydraulic that is capable of a wider range of test speeds and also longer crosshead displacements. The hydraulic machine is used much more when high forces must be applied. Electromechanical machines, are assembled from a variable speed electric motor, a gear reduction system, and one, two or four screws that move the crosshead upwards and downwards. Thus, the machine is able to perform tests of either compression or tension.

On the other hand hydraulic machines work in a different manner: Basically, a single or dual-acting piston moves the crosshead upwards or downwards and thus exerts greater forces on the specimen (Davis 2004).

2.7.1 Mechanical properties of a device derived from a tensile test

Tensile test is significant for the characterisation of the structural strength of a medical device. The tensile properties derived out of it, are needed for the quality improvement of a biomaterial or for the confirmation of a biomaterial quality. From the mechanical properties that are used for the description of a material (see subchapter 2.7) the tensile strength, yield strength, Young's module and ductility (elongation at break) will be described in detail. These will be used for the quality examination of the RRM as a candidate implant material and comparison with these properties of the non-welded specimens. Other mechanical properties (e. g. fatigue bending strength) are also important and should also be taken into consideration in a further investigation.

Tensile strength

The definition of tensile strength is “The ultimate tensile strength (UTS) or, more simply, the tensile strength, is the maximum engineering stress level reached in a tension test”. That means that brittle materials have tensile strength values near to the elastic limit and ductile materials have tensile strength values in the plastic portion of the stress-strain curve. Tensile strength values are qualified to determine the material type and also are useful for quality control of the materials. (NDT Resource Centre 2012)

Yield strength

Until yield point on a stress-strain graph a material obeys the Hooke’s Law (see Annex), where any elongation until yield point is reduced to its original value after the removal of the load without a permanent deformation. Yield point, is the point where a material changes from elastic to plastic deformation. Yield strength must not be mistaken for the yield point. “Yield strength is the stress required to produce a small-specified amount of plastic deformation. The yield strength obtained by an offset method is commonly used for engineering purposes because it avoids the practical difficulties of measuring the elastic limit or proportional limit”. (NDT Resource Centre 2012)

Young’s modulus

Young’s modulus is an important value, because it characterizes the stiffness of a material. Young’s modulus is defined as “the slope of the initial linear portion of the stress-strain curve”. (Davis 2004) Within the linear portion deformations are elastic, thus, the term modulus of elasticity is also used.

Ductility

Ductility is the elongation a material can withstand by deforming until fracture. Elongation and reduction of cross sectional area of the specimen are important values to state whether a material is brittle or ductile. Elongation or reduction in area is measured in percent and elongation is represented by the x-axis of a stress-strain graph.

Ductility can provide us with three main pieces of information: (a) what values a material can be extended and deformed without fracturing, (b) an indication of the flow of the material in plastic deformation before fracturing and (c) an indication of any impurities of the material or of any processing conditions which altered the structure of the material (Davis 2004).

CHAPTER III

Materials and Methods

The current experimental project took place in the medical university of Göttingen from February 2010 until February 2014 under the supervision of the biomaterial research sector of the orthopedic department. A pilot study was taken prior the valid experimental research. The materials used and the research design is described in detail below in this section.

3.1 Material description

The rectangular specimens used, were cut from a custom-made strap of ring mesh (F. Münch, Mühlacker, Germany). They were made of commercial pure (CP) titanium grade 4 and manufactured with a pattern of “4 in 1” where each ring holds four neighboring rings (Figure 2). The semi-finished product is a round wire with a thickness of 0.5 mm. Each ring has the following dimensions: outer diameter 4 mm, inner diameter 3mm. Important to say is that the circular form and the pattern of the rings are made after the bending of segments of wire and their two ends are welded by the manufacturer. A welded area is characterized by a small overlap and multicolored oxidation zone. Each ring weighs about 1 mg. Each specimen tested consisted of 138 rings and weighs around 1,4g. Furthermore the specimens have the following pattern: width 6 rings at the outside and five at the inside and also its length consists of 13 rings outside and 12 inside (Fig. 1). The contact area between the rings that was laser welded had the dimensions of 1,9mm length and 1mm width and about 1mm thickness and due to that it is considered to set the spot diameter of the laser at 1,9mm in order to apply the same energy to the contact area.

Figure 1

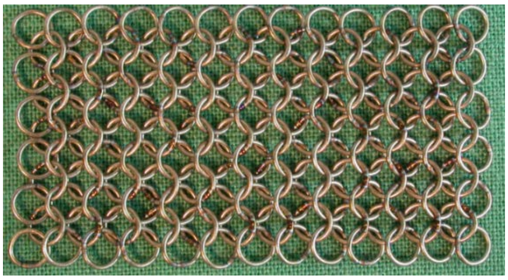

Non-welded specimen

Figure 2

Each ring is connected with four other rings

3.2 Material preparation

The specimens are prepared to have the same number of rings and thus the same dimensions. In pilot study, the samples were chemically cleaned in order to remove the alpha case (titanium oxide layer formed physiologically due to oxidation of the material) from the rings but the results of the pilot study indicated that the material was eroded and the welding procedure had as a consequence a porous welded region which was unable to withstand any tensile stress. With these observations the concerns about the influence of the alpha case in the material mechanical properties, were negligible if the material was not at all chemically cleaned. Thus, the experimental research of the specimens did not undergo any cleaning processes. The dimensions of the specimens were arbitrarily chosen to allow for an area of welded rings with balanced welding quality and to limit the number of welding points to a minimum. The assumption was made that the welding would weaken the tensile strength of the rings. Thus, failure of the non-welded rings would be less probable than failure within the welded area.

It was important to take into consideration the manufactured welding point (Figure 3) within a ring, where in a specimen these welding points have been accidentally distributed in the specimen. This played an important role in the mechanical properties of the material examined and is described in the results section of this dissertation.

Figure 3

Example of a manufactured welded point

3.3 Experimental equipment

The main equipment that was used in the experimental study was the Nd-YAG laser (Tanaka Laborlaser TLL 7000 Plus, Tanaka dental, Friedrichsdorf, Germany) and the universal test machine (Zwick 1446 with software testXpert Version 12.1, Zwick GmbH & Co. KG, Ulm, Germany).

The laser is equipped with a light tight housing, a protective argon gas supply is directed with hose pipes to the working place and a binocular lens focused on the intersection of two pointer laser beams directing to the working spot.
The laser beam can be configured by the parameters: current of the laser generator (A), duration of laser beam (msec), and diameter of laser beam at the working spot (mm). The actual energy applied to the welding site (J) depends on these parameters, as well as on the cleanliness of the optical elements. After inspection and service of the machine (Tanaka dental) the energy output was measured, and a short description is given in the subchapter research protocol.

Some modifications were made on these two equipment machines in order to perform the experiment correctly. The pilot tests, revealed that the original laser chamber was too large and the flow of protective argon gas via the hose pipes proved to be ineffective to prevent oxidation of the melt. On the laser equipment, was attached the modified part of the laser chamber, which was a nylon bag with a plexiglas opening at the bottom and an aluminum supporter at the top in order to hang on the laser equipment and the nylon bag to cover the x-y table with the lifting platform and the specimen. On both sides of the aluminum support, two connecting tubes allowed the argon gas from the laser to flow into the internal part. Thus, oxygen was minimized and the argon gas could cover and protect the welding area (Fig. 5). Furthermore the specimens were held vertically to the laser beam with a stretching device (Fig. 7), which could be orientated in all directions (lifting table and x-y table) (Fig. 6). The whole system was centralized in the laser chamber using magnets to keep it always centralized in the same position.

On the other hand, the opposing clamps of the tensile test machine were complemented with pairs of custom-made bronze brackets. These were characterized by a row of steel pins joined in the first and corresponding recesses in the second bracket. Each pin secured a ring of the non-welded first and final row. After closure of the clamp the recesses in the counter bracket supported the steel pins against bending (Fig. 4). The settings of the tensile test machine are listed in the Annex.

Figure 4

Modified clamp-brackets of the Zwick tensile test machine

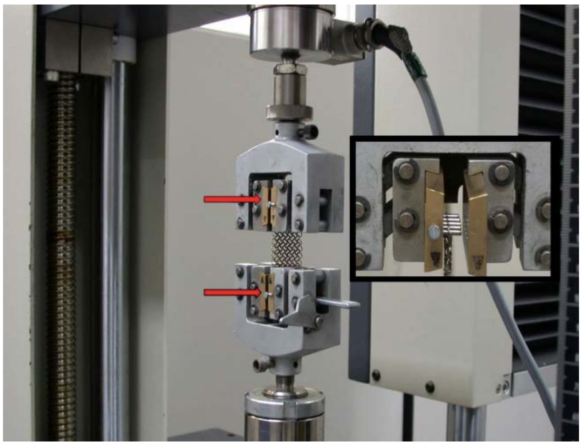

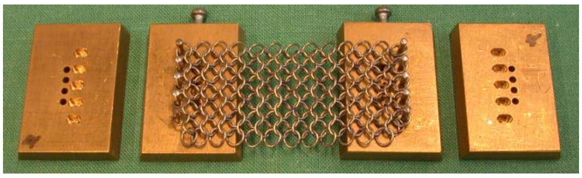

Welded mesh specimen held for testing in the clamps of the testing machine. Arrows point to the custom made bronze pieces

Figure 5

Laser chamber additional part with lift and cross table

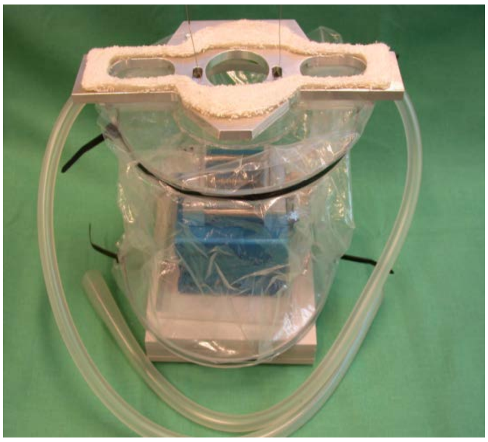

Additional device (curtain and fixation plate) to allow continually flow of argon gas in the welding area. The stretching device and the tables are enclosed by the curtain.

Figure 6

The x-y table combined with the lift table and the stretching device

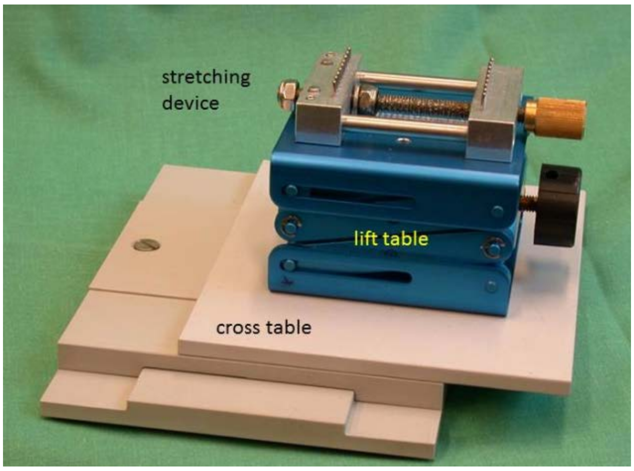

Figure 7

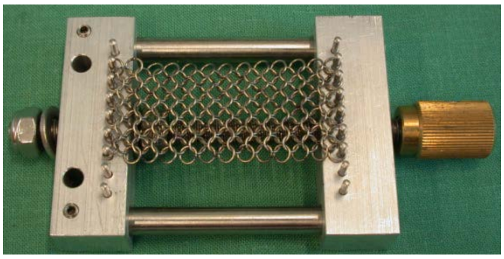

Figure 8

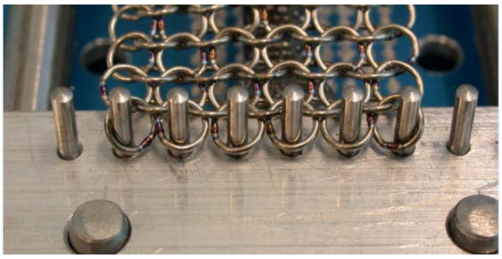

The stretching device with magnified view of the attached points

3.4 Research protocol

As already mentioned, this experimental project has been preceded by a pilot study where the specimens were chemically cleaned. The idea behind this action was to remove the oxide layer that is made on the surface of the titanium. The welding process, during the pilot study was done prior to the modification of the laser chamber. In total 50 specimens were cleaned and welded. The results, experiential macroscopically derived from the pilot study were important to observe that the cleaning of the titanium played an erosive role in the quality of the metal. In particular, macroscopically the welding points had no consistency, but they had porosity. In addition, the pilot study showed that another essential factor that influenced these results was the absence of a proper laser chamber and consequently the presence of oxygen that influenced the welding process.

Therefore, based on the results of the pilot study, the specimens were not cleaned in the experimental research in order to protect the quality of the metal. Secondly, a modification was necessary in the laser chamber, in order to avoid any presence of oxygen during the welding process and the flowing of inert argon gas, which is used originally from the laser to protect the material from the oxidation during the welding process. Each specimen has been treated equally under the same circumstances. The process is as follows: Firstly the specimen is tensioned with a special device until all the rings are stretched to make the whole length of the specimen. Then, it was adjusted on a lifting platform that was centralized on an x-y axis table in the middle of the laser chamber (this position was kept constant). Before the start of each welding procedure, the argon gas was allowed to flow for about two minutes, in order to remove the oxygen. During the welding procedure, the argon gas flows continuously until the last welding point. The specimens have been welded at room temperature. The spot diameter was kept constant at 1.9 mm, which are the dimensions of the contact points. The industrial production welding points in a ring, which is made during the manufacture of the mesh, are taken into consideration as they probably have undergone altered crystalline structure. These were kept randomly distributed in the specimen, where they either intersect in some points with the welded area between the rings or not. The specimens were welded with a unique technique, where every second row was welded. This process was done for two reasons. The first reason is to avoid the overheating of the one central ring and also to give it the necessary cooling time. The second reason was to not change the height of the specimen since the form of the specimen is a zig-zag shape if it is seen from a transverse section angle. Thus, the centralization and the calibration were not changed and it was used identically for every single welding point. Due to the fact, that the contact points had a diameter of 1 mm, the welding process followed was a heat conduction welding, whereas this type of welding is used for micro welding of metals less than 2mm. The same process was applied also for the other side of the specimen. The reason for welding the specimen from both sides is to control the heat conduction welding instead of giving a huge energy to the welding area (deep penetration welding). It is worth mentioning, that during all research procedures, the specimens were welded from both sides with one laser shot in every contact area. Only the rows at each end of the specimen were not welded for attachment of the specimen on the bronze clamp parts of the tensile test machine.

This procedure has been done under the use of the binocular lens and the consistency of the extension, position and mirror surface of all welded points was microscopically evaluated. The high adjustability range of the laser parameters, such as the current and impulse duration was the most challenging part in the experimental work. In order to find out, which combination between these two parameters would provide the best results, the following mind scheme was made. The experimental work, was divided into four phases: the Phase A which was subdivided into Part 1 and Part 2, Phase B, Phase C (step 1 and step 2) and Phase D. Phase A intended to indicate the range for optimum laser parameters (Energies) that results in acceptable welding status for the RRM. Using an energy diagram in Phase B aimed to assess the energy values and to confirm high quality welding results. In Phase C, the aim was to compare in step 1 the mechanical properties between the lower energy values found in Phase B with the non-welded specimens and in step 2 to compare if there are any differences between laser parameters providing the same energy values. Phase D was the last step of the experiment, which compared the mechanical properties between different energy levels.

In Part 1 of the Phase A, the independent variables used were the current (independent variable 1) and the impulse duration (independent variable 2), where the current was kept constant at 210A, which is the median value of the range given (100A – 320A). The independent variable 2, namely the impulse duration, was changed every one unit starting from 1ms to 15ms. Therefore, in Part 1 a total of fifteen specimens (815 welding points) were welded by using these variable values. Then the welded specimens were tested individually and underwent the sequent examinations.

The test examined the following four dependent variables: dependent variable 1 was ‘Tensile Strength’, dependent variable 2 was ‘Elongation at break’ (Ductility), dependent variable 3 was ‘Young’s modulus’ and dependent variable 4 was ‘Yield strength’.

In Part 2 of the Phase A, the controlled experiment was performed like in Part 1 with the only difference that the independent variable 2 was kept constant at 8ms (median value of the range 1ms-15ms). The independent variable 1 was changed every 20 units from 100A to 320A but at the range of 160A to 180A (which was the range with the acceptable welding energy values) was changed every 5 units to optimize the results. Totally in Part 2 also fifteen specimens (815 welding points) were welded. As in Part 1, the ‘acceptable welded’ specimens undertook tensile test and the following dependent variables were tested: dependent variable 1 ‘Tensile Strength’, dependent variable 2 ‘Elongation at break’ (Ductility), dependent variable 3 ‘Young’s modulus’ and dependent variable 4 ‘Yield strength’. The tensile test results of Phase A were compared with the control group (non-welded specimens).

In Phase B, the energy values given from the laser manufacturer (Mr. Turek,Tanaka laser, Ulm) were extrapolated in an energy graph and it was used to confirm, whether the energy values derived from Phase A were within the expected range. For each dataset of energy values at given time pulse and current registered by the Laser manufacturer, a linear dependence between Energy and Current for a given time pulse was observed. Therefore, a linear regression approach, the chi-square method was used to fit and extrapolate the observed data. Using the fitting results one can derive information at higher energies. These energy values were not provided by the manufacturer, due to the fact that the joule meter could not withstand higher energy values.

The quantity χ^2/NDoF is used as the goodness of fit of the linear model and characterizes how well the set of observations is fit. More specifically, the output of the chi square (χ^2) is normalized to the number of degrees of freedom (NDoF), in our case the number of the experimental points of each dataset.

An attempt has been made to extract values for times that the manufacturer did not provide (Fig. 14). So for times 5ms–12ms the lines of the graph are drawn based on interpolation of the fit data. However, the interpolations are associated by large uncertainties and therefore are not exclusively used to make final decisions.

The error on the energy was calculated using propagation of errors of the chosen working points (see equation annex).

Furthermore, Phase C was subdivided into two steps. In step 1, the goal was to compare the mechanical properties between the lowest energy value and the non-welded specimens. Step 2 was done to compare, whether the tensile results of parameter combination for the same energy level could give the same statistical results.

On the other hand in Phase D, what was tested was the statistical difference of the tensile results between specimens of the highest and lowest energy values.

For the procedure the Statistical Package for the Social Sciences (SPSS) (IBM Corp. 2012) was employed to analyze the primary quantitative data of the study. In particular, the independent t-test was used to identify statistical significant differences.

CHAPTER IV

Results

4.1 Phase A

In Part 1 of Phase A, the current was kept constant at 210A (the median value of the given current range) and the time was increased one unit (1ms) every time starting from 1 ms to 15ms. Of the total of fifteen specimens only two of them were acceptably welded. In particular, acceptable welding was achieved at 5ms and 6ms. The remaining thirteen were ‘unacceptably welded’ (textured welding area). Therefore, they were excluded from the tensile test. As can be seen in Table 1, there are not huge differences regarding the mechanical properties of the two acceptable welded specimens of Part 1.

Table 1

Results of the tensile test in Phase A- Part 1

Current (A)	Impulse duration (ms)	Welding status	Tensile strength (MPa)	Elongation at break (%)	Young's modulus (MPa)	Yield strength (MPa)
210	1	1	-	-	-	-
	2	1	-	-	-	-
	3	1	-	-	-	-
	4	1	-	-	-	-
	5	2	62,80	8,39	2157	17
	6	2	64,05	9,91	2026	17
	7	3	-	-	-	-
	8	3	-	-	-	-
	9	3	-	--	-	-
	10	3	-	-	-	-
	11	3	-	-	-	-
	12	3	-	-	-	-
	13	3	-	--	-	-
	14	3	-	-	-	-
	15	3	-	-	-	-

815 welding points including the two samples with acceptable welding energy. Welding status: 1=low energy thus no weld, 2=optimum energy for acceptable weld, 3= very high energy that leads to separation of the material.

Figure 9

Stress-strain curve

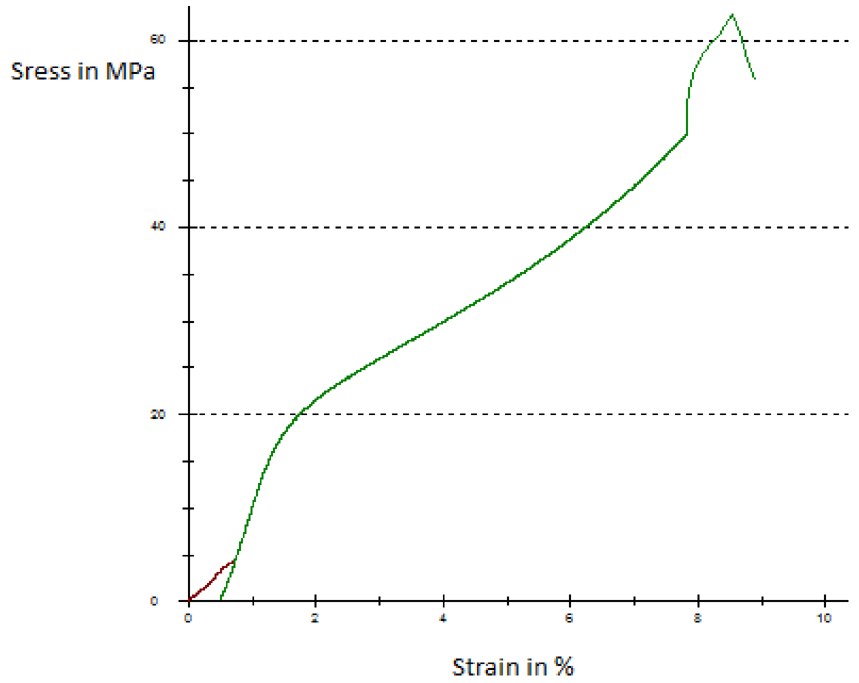

Phase A - Part1 210A-5ms welded

Figure 10

Stress-strain curve

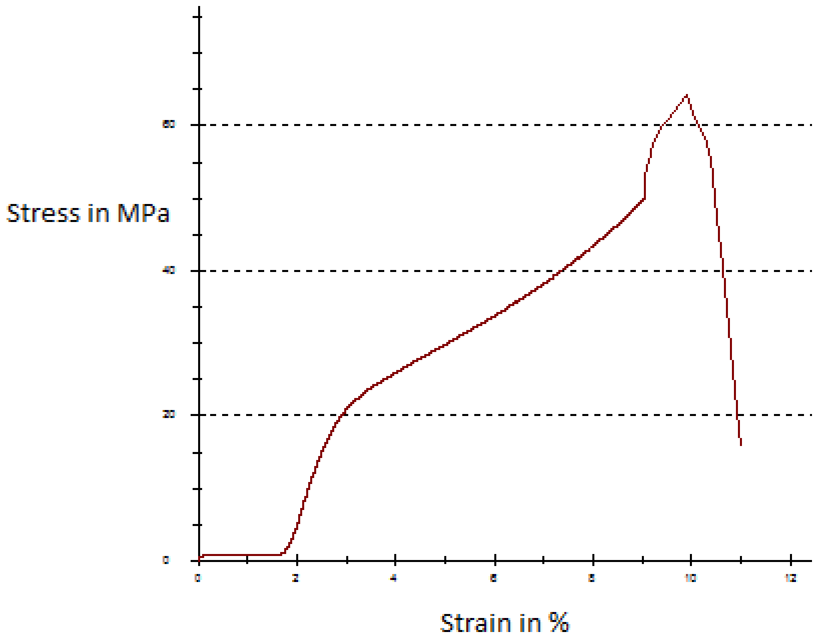

Phase A - Part1 210A-6ms welded

Figure 11

Stress-strain curve

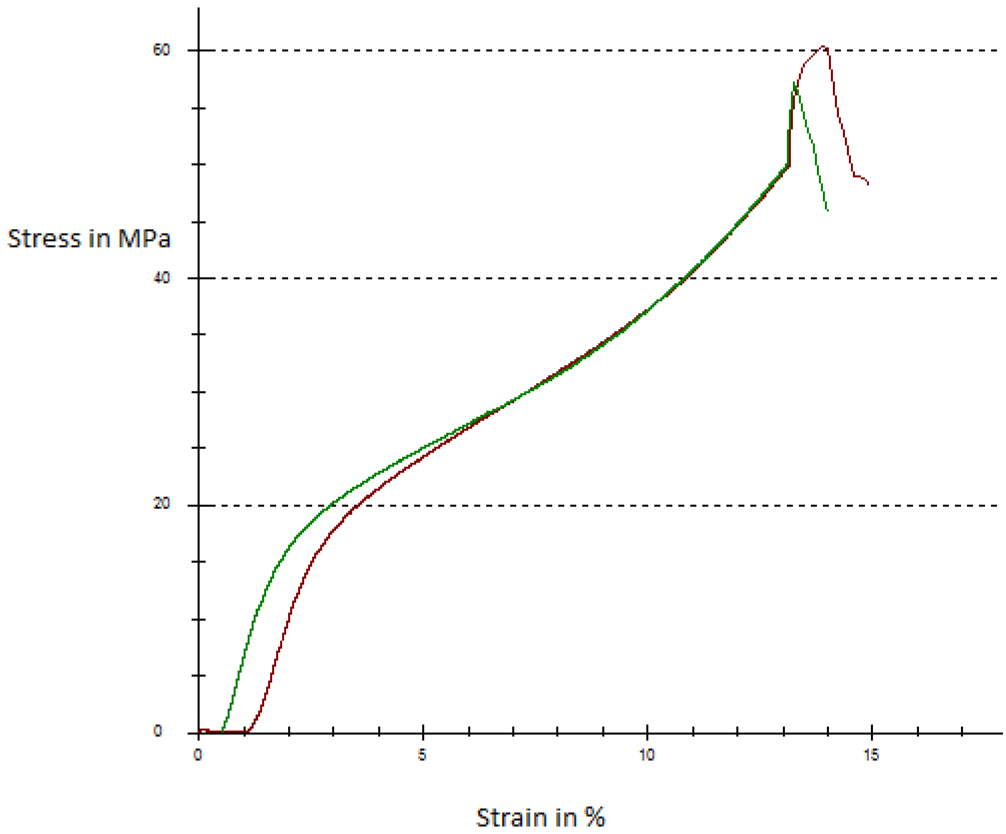

Phase A - Part1 non-welded

In the second part of Phase A, the impulse duration was kept constant at 8ms (the median of the given time range) and as already mentioned, the current was increased 20 units every time; however, in the range of 160A – 180A with the most optimal laser energy the current was increased every 5 units. As in Part 1, only two of the fifteen specimens were ‘acceptably welded’, thus the remaining specimens were excluded from the tensile test. The ‘acceptable welded’ specimens were welded at current values 170A and 175A accordingly. From the tensile test results, as shown in Table 2, the mechanical properties of the specimens of the two parts fluctuated in the same range.

Figure 12

Stress-strain curve

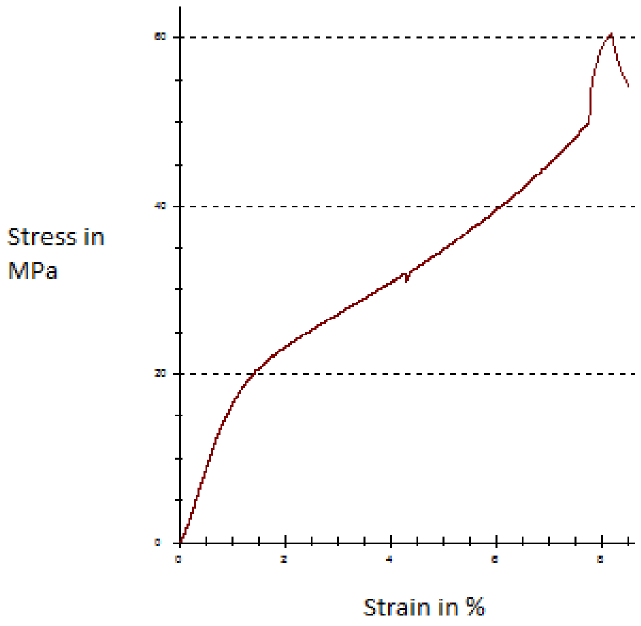

Phase A - Part2 170 A - 8 ms welded

Figure 13

Stress-strain curve

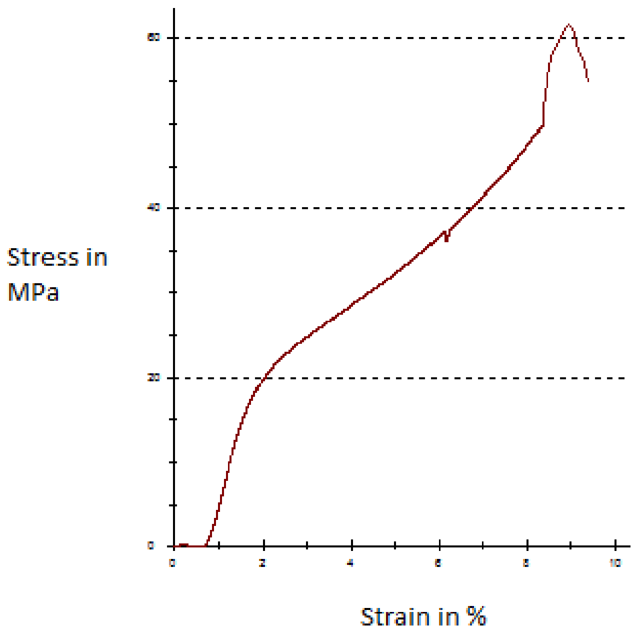

Phase A – Part 2 175 A 8 ms welded

Table 2

Results of the tensile test in Phase A- Part 2

Current (mA)	Impulse duration (ms)	Welding status	Tensile strength (MPa)	Elongation at break (%)	Young module (MPa)	Yield strength (MPa)
100		1	-	-	-	-
120		1	-	-	-	-
140		1	-	-	-	-
160		1	-	-	-	-
165		1	-	-	-	-
170		2	60,48	8,53	1959	18
175		2	61,80	9,39	2144	16
180	8	3	-	-	-	-
200		3	-	-	-	-
220		3	-	-	-	-
240		3	-	-	-	-
260		3	-	-	-	-
280		3	-	-	-	-
300		3	-	-	-	-
320		3	-	-	-	-

815 welding points including the two samples with acceptable welding energy. Welding status: 1=low energy thus no weld, 2=optimum energy for acceptable weld, 3= very high energy that leads to separation of the material.

4.2 Phase B

From the observations extracted in Phase A, the hypothesis arose that there was a fluctuation of energy values regarding the different laser parameters. In order to verify this hypothesis, it was necessary to find out the energy values by different laser parameters. As stated in subchapter Research protocol a joule meter was used. A graph was plotted of Energy (J) versus Current (A) at different impulse durations (ms). The laser parameters determined in Phase A were found to be in the field of Energy versus Current graphs with appropriate energies in the range of 12 to 15J (see Fig. 14). It was then verified with experimental work and microscopic evaluation, using different laser parameters in between 12J and 15J whether there was an acceptable or a non-acceptable welding status. From the experiments, it is proved that acceptable welding status fluctuates in the energy range 12J and 15J.

It is worth mentioning that Figure 21 was designed using the data given by the direct registration of some values collected by the joule meter from the laser manufacturer in my presence. Nevertheless, the manufacturer provides data only regarding the impulse durations (time) between 1-4ms.

For each dataset, a linear dependence between Energy and Current for a given time was observed. Therefore, a linear regression approach, the chi-square method was used to fit and extrapolate the observed data. Using the fitting results one can derive information at higher energies. The manufacturer did not provide these energy values, due to the fact that the joule meter could not withstand higher energy values.

The quantity χ^2/NDoF is used as the goodness of fit of the linear model and characterizes how well the set of observations is fit. More specifically, the output of the chi square (χ^2) is normalized to the number of degrees of freedom (NDoF), in our case the number of the experimental points of each dataset.

In figure 21, an attempt has been made to extract values for times that the manufacturer did not provide. So for times 5ms–12ms the lines of the graph are drawn based on interpolation of the fit data. However, the interpolations are associated with large uncertainties and therefore are not exclusively used to make final decisions.

The error on the energy was calculated using propagation of errors of the chosen working points (see equation annex). Consequently, for the purposes of the following procedures, impulse durations were used close to 4 ms, in order to minimize the errors.

Figure 14

Energy diagram

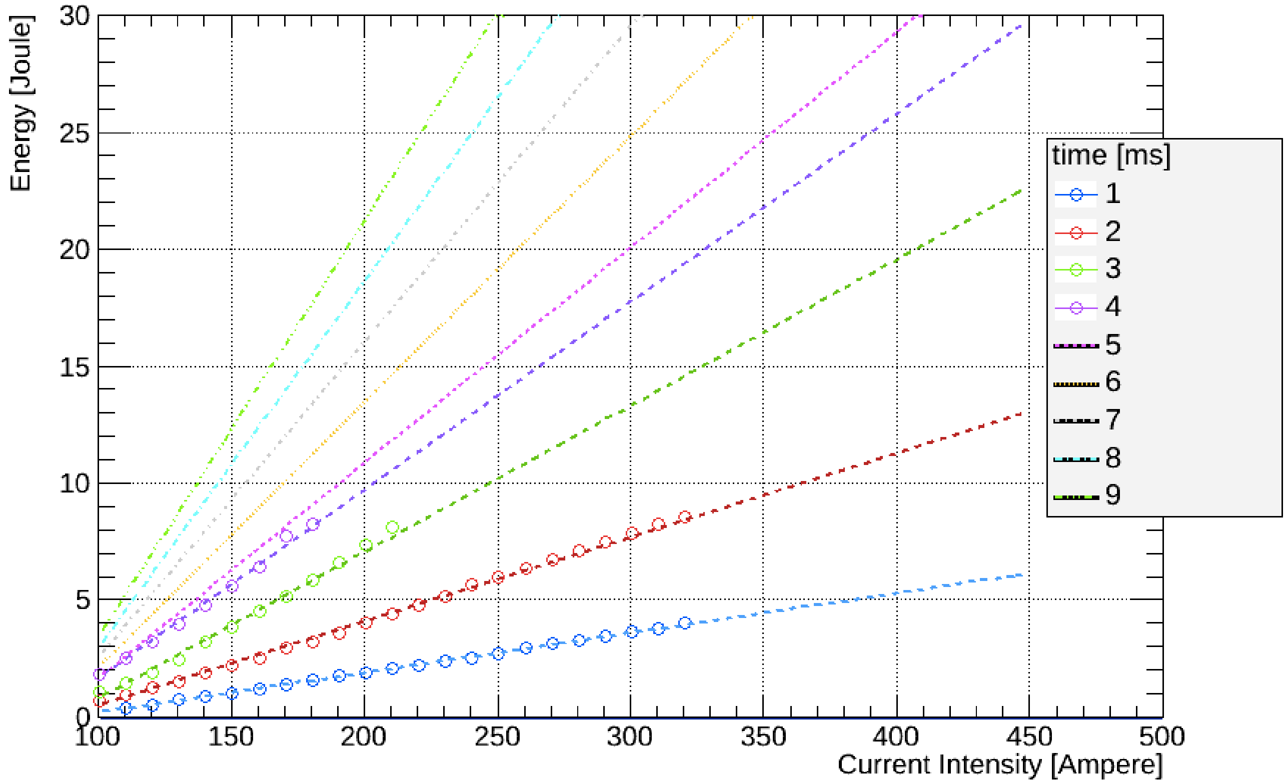

Figure 14: Experimental data provided by the manufacturer are represented with open circles at different times and indicated by different colors. Each experimental data set is fit by a linear model shown with dashed lines. The lines lacking overlaid data are simply interpolations.

4.3 Phase C

Phase C, attempted to assess the consistency and reliability of quality results by comparing the welded specimens with non-welded specimens, as well as by comparing two groups of welded specimens that received the same laser energy values, but with a different set of laser parameters.

In the first part of the third phase, the Experimental Group was recruited consisting of four specimens (1600 welding points) that were welded with the energy value of 12J and specifically by using the combination of current 210A and impulse duration 5ms. The four specimens of the experimental group as well as the four non-welded specimens comprising the control group, underwent the tensile test and resulted in the findings that are shown in Table 3 and Figure 15.

Table 3

Results of the tensile test in experimental & control group

	Experimental Group – Welded (210A-5ms)				**Control Group – Non-welded**			
Specimen No./ Mechanical Properties	1	2	3	4	1	2	3	4
Young's Modulus (MPa)	2125	2255	2038	2156	1287	1234	1208	1299
Tensile Strength (MPa)	62.58	65.04	63.05	61.92	60.41	57.26	62.12	61.09
Elongation at break (%)	7.4	7.8	8.0	7.7	14.96	13.53	12.72	15.11

In addition, using the statistical software SPSS, the mechanical properties of the four welded specimens were statistically compared with the mechanical properties of the four non-welded specimens (control group). Firstly, the normality of the data was tested. The Shapiro – Wilk test (see Table 4) revealed that the Young's modulus, tensile strength and elongation at break are normally distributed for each group of the independent variable (see also the normal Q-Q Plots, Plots 1 - 6 in Annex). The yield strength was excluded from the following research procedures because the value for all specimens was 17MPa where this was not an essential factor to analyze.

Figure 15

Stress-strain curve of the experimental group (210A – 5ms)

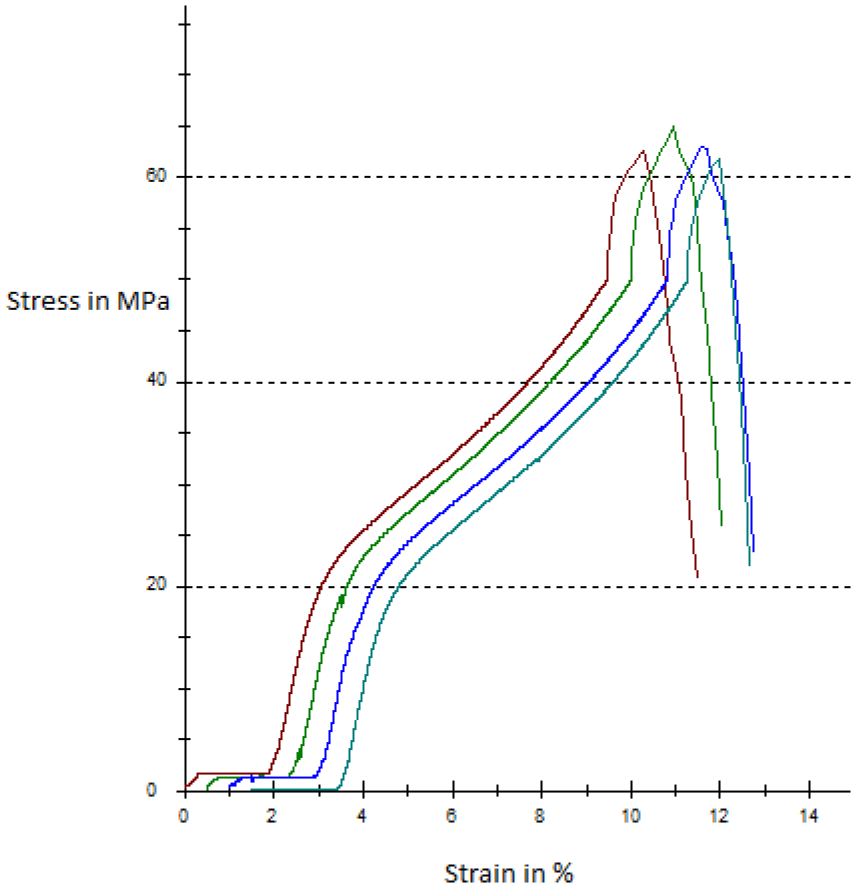

The graphs are shifted for visual purposes

Table 4

Test of Normality

	Control Group or Experimental Group	Shapiro-Wilk		
		Statistic	df	Sig.
Young' s Modulus (MPa)	Control Group	,910	4	,484
	Experimental Group	,989	4	,954
Tensile Strength (MPa)	Control Group	,906	4	,461
	Experimental Group	,911	4	,489
Elongation at break (%)	Control Group	,887	4	,368
	Experimental Group	,982	4	,911

Test of Normality (Shapiro – Wilk test, SPSS statistical software)

Then, the independent t-test (see Tables 5 - 6) was employed to identify possible statistically significant differences between the two groups. As was expected, the test revealed that there were statistically significantly higher values regarding the parameter of Young's modulus in the experimental group (2143.5 ± 89.86 MPa) than in the control group (1257 ± 43.18 MPa) (t(6)= 17.833, p=0.00). Furthermore, statistically significantly lower values were recorded regarding the elongation at break in the experimental group (7.72 ±0.25%) than in the control group (14.08 ± 1.15%) (t(3.282)= 10.774, p = 0.001). These results, were not unexpected, because the welded specimens did not retain their elasticity that they had before welding. The findings also indicated that there was no statistically significant difference between welded and non-welded specimens regarding the tensile strength, t(6)= 2.352, p=0.057. Therefore, the results were in favor of experimental group (experimental group: 63.15 ±1.34 MPa and control group: 60.22 ±2.09 MPa).

Table 5

Group statistics: Welded (Experimental)-Non-Welded (Control)

Group Statistics

	Group	N	Mean	Std. Deviation	Std. Error Mean
Young' s Modulus (MPa)	Control Group	4	1257,0000	43,18179	21,59089
	Experimental Group	4	2143,5000	89,55631	44,77816
Tensile Strength (MPa)	Control Group	4	60,2200	2,09480	1,04740
	Experimental Group	4	63,1475	1,34411	,67205
Elongation at break (%)	Control Group	4	14,0800	1,15288	,57644
	Experimental Group	4	7,7250	,25000	,12500

Table 6

Independent samples test: Welded- Non-welded

Independent Samples Test

		Levene´s Test for Equality of Variances		t-test for Equality of Means						
									95% Confidence Interval of the Difference	
		F	Sig.	t	df	Sig. (2-tailed)	Mean Difference	Std. Error Difference	Lower	Upper
Young' s Modulus (MPa)	Equal variances assumed	,892	,381	-17,833	6	,000	-886,5000	49,71167	-1008,14007	-764,85993
	Equal variances not assumed			-17,833	4,323	,000	-886,5000	49,71167	-1020,54359	-752,45641
Tensile Strength (MPa)	Equal variances assumed	,548	,487	-2,352	6	,057	-2,92750	1,24447	-5,97261	,11761
	Equal variances not assumed			-2,352	5,112	,064	-2,92750	1,24447	-6,10551	,25051
Elongation at break (%)	Equal variances assumed	18,058	,005	10,774	6	,000	6,35500	,58984	4,91172	7,79828
	Equal variances not assumed			10,774	3,282	,001	6,35500	,58984	4,56577	8,14423

The second part of Phase C aims to compare two groups of specimens that were welded with the same energy value, but by using different set of laser parameters. Particularly, two sets of parameters were used: current 210A and impulse duration 5ms (as already used in Part1) and the combination of: current 280A and impulse duration 3ms, which both result energy of 12J. The results of tensile test of both combinations are illustrated in Table 7. As can be seen in the table below, there are no large discrepancies between the two groups, especially regarding Young's modulus and Tensile strength.

Table 7

Results of the tensile test in two groups of laser energy 12J

	Laser Energy of 12J							
	Welded with 210A-5ms				**Welded with 280A-3ms**			
Specimen No./ Mechanical Properties	1	2	3	4	1	2	3	4
Young's Modulus	2125	2255	2038	2156	2117	2235	2271	2221
Tensile Strength	62.58	65.04	63.05	61.92	62.23	57.52	64.15	57.69
Elongation at break	7.4	7.8	8.0	7.7	8.80	8.21	8.63	8.08

After assessing that the dependent variables were normally distributed in each combination of laser parameters (see: Table 8 and Plots 7-12 in Annex), the independent t-test (see Tables 6-7) was used to detect possible statistically significant differences between the two groups. The Tables 9 and 10 depict that there were not statistically significant differences between the two combinations regarding the mechanical properties of Young's modulus and Tensile strength ($p>0,05$). There were observed statistically significantly higher values of Elongation at break in the group of specimens welded with the laser combination of 280A-3ms (8,43±0,34%) than in the group welded with 210A-5ms (7,73±0,25%), proving that the former has generally more elasticity than the latter ($t\ (6)=3.338$, $p=0,016$). Compared to the non-welded specimen the RRM produced with 280 A and 3 ms (12 J) in principle did not differ from those RRM produced with lower current and longer pulse duration.

Table 8

Test of Normality

	Combinations at 12J	Shapiro-Wilk		
		Statistic	df	Sig.
Young' s Modulus (MPa)	210A-5ms (12J)	,989	4	,954
	280A-3ms (12J)	,892	4	,394
Tensile Strength (MPa)	210A-5ms (12J)	,911	4	,489
	280A-3ms (12J)	,854	4	,238
Elongation at break (%)	210A-5ms (12J)	,982	4	,911
	280A-3ms (12J)	,917	4	,519

Table 9

Group statistics: 12J (210A-5ms) – 12J (280A-3ms)

Group Statistics

	Combinations at 12J	N	Mean	Std. Deviation	Std. Error Mean
Young' s Modulus (MPa)	210A-5ms (12J)	4	2143,5000	89,55631	44,77816
	280A-3ms (12J)	4	2211,0000	66,11102	33,05551
Tensile Strength (MPa)	210A-5ms (12J)	4	63,1475	1,34411	,67205
	280A-3ms (12J)	4	60,3975	3,31913	1,65957
Elongation at break (%)	210A-5ms (12J)	4	7,7250	,25000	,12500
	280A-3ms (12J)	4	8,4300	,34049	,17024

Table 10

Independent samples test: 12J (210A-5ms) – 12J (280A-3ms)

Independent Samples Test

		Levene´s Test for Equality of Variances		t-test for Equality of Means						
									95% Confidence Interval of the Difference	
		F	Sig.	t	df	Sig. (2-tailed)	Mean Difference	Std. Error Difference	Lower	Upper
Young' s Modulus (MPa)	Equal variances assumed	,208	,664	-1,213	6	,271	-67,50000	55,65743	-203,68884	68,68884
	Equal variances not assumed			-1,213	5,521	,275	-67,50000	55,65743	-206,60476	71,60476
Tensile Strength (MPa)	Equal variances assumed	11,067	,016	1,536	6	,175	2,75000	1,79048	-1,63114	7,13114
	Equal variances not assumed			1,536	3,958	,200	2,75000	1,79048	-2,24195	7,74195
Elongation at break (%)	Equal variances assumed	1,652	,246	-3,338	6	,016	-,70500	,21121	-1,22180	-,18820
	Equal variances not assumed			-3,338	5,506	,018	-,70500	,21121	-1,23325	-,17675

4.4 Phase D

Finally, the last phase intended to compare specimens that were welded with different laser energies. Particularly, specimens were used that were welded with the minimum 'acceptable' welding energy of 12J as well as with the maximum 'acceptable' energy of 15J. Regarding the energy of 12J, the laser combination of 280A and 3ms and for the group of 15J the laser combination 320A and 3ms was used. These combinations, were chosen because based on the energy diagram illustrated in Phase B at impulse duration 3ms it was possible to take a set of laser parameters that could have the least propagation of error. The propagation of error at 280A/3ms is (12.06J ±2.19) and for 320A/3ms is (14.57 ±2,81). Four specimens of each group were tensile tested and the findings are represented in the Table 11.

Table 11

Results of the tensile test in the groups of laser energy 12J and 15J

	Laser Energy of 12J				**Laser Energy of 15J**			
	Welded with 280A-3ms				**Welded with 320A-3ms**			
Specimen No./ Mechanical Properties	1	2	3	4	1	2	3	4
Young's Modulus	2117	2235	2271	2221	2204	2126	1994	2252
Tensile Strength	62,23	57,52	64,15	57,69	44,17	54,17	50,63	49,62
Elongation at break	8,80	8,21	8,63	8,08	6,39	7,87	7,36	7,30

Subsequently, the independent t-test was run to determine if there were differences in the mechanical properties between the specimens welded with 12J and 15J. As assessed by Shapiro Wilk test ($p>0,05$) the three mechanical properties were normally distributed for each laser energy level (see Table 12 and Plots 13-18, Annex). It can be seen from the data in the tables 13 and 14 that there was no statistically significant difference between the two groups regarding Young's modulus. However, concerning the Tensile strength and Elongation at break, there were recorded statistically significantly higher values in the group of the specimens welded with 12J (60,40 ±3,32 MPa and 8,43 ±0,34%, respectively) than those with 15J (49,65 ±4,14MPa and 7,23 ±0,62%, respectively) . (For Tensile strength: t(6)=4.052, p=0.007 and for Elongation at break: t(6)=3,411, p=0.014). The results demonstrate that the specimens welded with 12J were in general harder and more elastic than the specimens that received welding energy 15J.

Table 12

Test of Normality

	12J - 15J	Shapiro-Wilk		
		Statistic	df	Sig.
Young's Modulus (MPa)	280A-3ms (12J)	,892	4	,394
	320A-3ms (15J)	,951	4	,720
Tensile Strength (MPa)	280A-3ms (12J)	,854	4	,238
	320A-3ms (15J)	,964	4	,804
Elongation at break (%)	280A-3ms (12J)	,917	4	,519
	320A-3ms (15J)	,928	4	,582

Table 13

Group statistics: 12J & 15J

Group Statistics

	12J or 15J	N	Mean	Std. Deviation	Std. Error Mean
Young's Modulus (MPa)	280A-3ms (12J)	4	2211,0000	66,11102	33,05551
	320A-3ms (15J)	4	2144,0000	112,67653	56,33826
Tensile Strength (MPa)	280A-3ms (12J)	4	60,3975	3,31913	1,65957
	320A-3ms (15J)	4	49,6475	4,14013	2,07007
Elongation at break (%)	280A-3ms (12J)	4	8,4300	,34049	,17024
	320A-3ms (15J)	4	7,2300	,61563	,30781

Table 14

Independent samples test: 12J & 15J

Independent Samples Test

		Levene´s Test for Equality of Variances		t-test for Equality of Means						
		F	Sig.	t	df	Sig. (2-tailed)	Mean Difference	Std. Error Difference	95% Confidence Interval of the Difference Lower	95% Confidence Interval of the Difference Upper
Young's Modulus (MPa)	Equal variances assumed	1,162	,323	1,026	6	,345	67,00000	65,31973	-92,83161	226,83161
	Equal variances not assumed			1,026	4,847	,353	67,00000	65,31973	-102,51999	236,51999
Tensile Strength (MPa)	Equal variances assumed	,001	,978	4,052	6	,007	10,75000	2,65317	4,25792	17,24208
	Equal variances not assumed			4,052	5,729	,007	10,75000	2,65317	4,18274	17,31726
Elongation at break (%)	Equal variances assumed	,481	,514	3,411	6	,014	1,20000	,35176	,33928	2,06072
	Equal variances not assumed			3,411	4,678	,021	1,20000	,35176	,27675	2,12325

All the specimens were investigated after the tensile test and all of them follow the same breakage attribute. A broken RRM specimen after the tensile strength test is shown in Figure 16. As can be seen, the welded regions are sufficiently welded and the fractures were predominantly located at non-welded parts of the rings. Neither the industrially formed welds of single rings, nor the experimentally produced welds of contact areas were of mechanical strength inferior to the wire material.

Besides that, the rings seem to gain in length and deform in such an extent without easily breaking. The contact area welds appear to maintain their geometry and their concave oriented deformation occurs on the longitudinal directed parts of a ring. Lengthening of the specimen predominantly occurs on the traversely orientated parts of the rings. This aspect indicates the elasticity of the material and the ability of the welded region to withstand great forces.

Figure 16

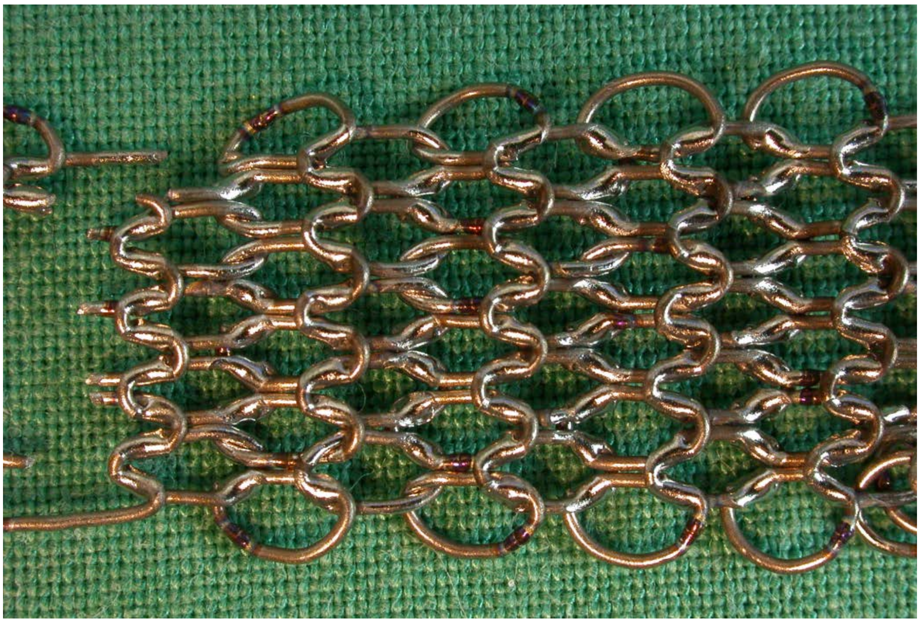

A welded specimen after a tensile strength test.

CHAPTER V

Discussion

It is a fact that titanium mesh is used in maxillofacial reconstructive surgery. According to Lazaridis et al.: 'Titanium mesh has proved a useful material for semi-rigid fixation and reconstruction of craniofacial defects'. In addition, it is stated: 'The semi-rigid fixation achieved by the malleable titanium mesh improves bone healing because of the micro movements at the fractured ends while rigid plates may evoke stress-forces within the callus during its formation and in the mass of the bone causing ischaemia under the area of the plate' (1998, p. 227). Other benefits for using titanium mesh are that it does not produce many artefacts in CT scan and also it does not migrate because connective tissue grows through and around its lattice structure (Lazaridis et al. 1998).

The RRM also has advantages over already existing titanium mesh. Despite that, the already existing mesh mentioned above differs from the RRM in that the RRM has the ability, due to its elastic character to be tucked during surgery and be applied in complex anatomical bone areas, which would be impossible for any other medical device. In addition, the RRM can be manufactured in a variety of medical devices in which the variation of the material cross-sectional area gives an alteration to the tensile strength more than the variation of the ring diameter. This production possibility gives an advantage to the RRM in contrast to the already existing 2D plates.

At the beginning of this experimental project, five research questions were raised which have been answered at the end of this experimental work. The first research question was the following: (a) Is it at all possible to provide a medical device using the RRM? The RRM introduces an idea of how every bone defect and not only maxillofacial traumata can be surgically treated. The difficult part was to provide a medical device, which with required mechanical properties can give the flexibility and at the same time the strength needed to stabilize the damaged area. At present the RRM used has arbitrary dimensions and are an example for future applications. Similar to the experiments presented here the welding parameters will have to be adjusted to differently dimensioned rings and modifications of the mesh pattern. According to the results it will be possible to shape the RRM according to a given anatomical structure by laser welding and apply it as an implant in the human body.

The second research question was: (b) Does the laser welding process work effectively to produce a stable medical device? According to the literature review done prior to the experimental work, the latest method used for welding process not only in different disciplines in the field of sciences but predominantly in routine manufacturing is the use of laser equipment. Using this knowledge the Nd-YAG laser was used to weld the specimen's contact points. The specimens were welded with a unique technique, where every second row was welded. This process was done for two reasons. The first reason is to avoid the overheating of the one central ring and also to give it the necessary cooling time. The second reason was to not change the height of the specimen since the form of the specimen is a zig-zag shape if it is seen from a transverse section angle. Thus, the centralization and the calibration were not changed and it was for every single welding point identically used. Due to the fact that the contact points had a diameter of 1mm the welding process followed was a heat conduction welding, whereas this type of welding is used for micro welding of metals. The same process was applied also for the other side of the specimen. The reason for welding the specimen from both sides is to control the heat conduction welding instead of giving a huge energy to the welding area (deep penetration welding). Intermittent and two-sided welding of the stretched RRM resulted in two-dimensional devices free of distortion. Though the character of the flexible RRM has been completely changed towards a stiffer device, only the welding process has produced a material applicable to stabilization procedures for surgery. This approach to the welding process was theoretically investigated prior to any experimental work. This theoretical model with the intention to achieve a sufficient welding area was verified with the results of the experimental work. Thus, it comes to the conclusion that this experimental approach is needed to produce the same good quality of any future work with rings of different dimensions.

In addition, another question that rises in the considerations of the project was the following: (c) What is the optimum energy applied on the contact points? This part of the study was the most challenging. The variable laser parameters, such as current and impulse duration should be varied in such a way in order to find the best combination of the two parameters that should present the best welding results with macroscopic and microscopic homogeneity and optimum mechanical properties. The goal of the process was to achieve also a conduction heat welding and not deep penetration welding process. That means, for a single welding point is needed a sum of energy 24J-30J since the specimens are welded from both sides. Using the mind scheme, explained in the method section of this dissertation, it is confirmed by the results of the study that the mind scheme is correct and assigned the best results. On the other hand, using this method for welding the medical device could answer automatically also the fourth research question revealed at the beginning of the study, which was: (d) Does the optimum laser parameters provide reliable mechanical properties results? The findings support the predictions, that the mechanical properties results using the laser parameters that provide energies between 12J and 15J (one side welding) under the same conditions (centralization of the cross table and time of argon flow at room temperature) disclose the best possible axial tensile test results. Well worth mentioning is the avoidance of using energy values from the energy graph, which are above the 4ms. Those values, above 4ms are an interpolation of the energy diagram for demonstration reasons of the energy. The reason for that is the considerable wide range of the standard error that would lead to false welding energy values. It is also to perceive, that in any future experimental work there is no need to descale (remove the alpha-case) or clean in any chemical way the RRM specimens, where such an action would may lead to erosion of the metal and thus to false tensile strength results. Another question that was recorded at the beginning of the experimental project was, if there are any differences between the tensile strength of the welded and non-welded specimens. In the literature review the molecular structure of titanium was studied in detail and it was noticed that the metallographic properties of pure titanium is of alpha phase, defined as "**Alpha alloys**". "These are non-heat treatable and are generally very weldable. They have low to medium strength, good notch toughness, reasonably good ductility and have excellent properties at cryogenic temperatures" (Materials Information Service 1995) and at temperatures of about 882^{o}C changes its metallographic properties to alpha-beta phase which is defined as "**Alpha-Beta alloys".** "These are heat treatable to varying extents and most are weldable with the risk of some loss of ductility in the weld area. Their strength levels are medium to high" (Materials Information Service 1995). And a beta phase is defined as "**Beta alloys".** "Beta or near beta alloys are readily heat treatable, generally weldable, and offer high strength up to intermediate temperature levels" (Materials Information Service 1995). Having this scientific knowledge in mind one struggled to find the "golden mean" in order to not use laser parameters to such an extent that could result in raising the temperature of welding points around 882^{o}C during the welding process. According to the results of the project, the welded and non-welded specimens do not differ from each other and from the results it is possible to say that the welded specimens reached temperatures around 882^{o}C, where that made a possible crystallographic change of the material to a metallographic state of alpha-beta alloys, where there is some loss of ductility and the strength levels are medium to high.

Inspection of the welding points revealed no significant variabilites, though the shifting table was manually driven. Fractures were predominantly located at non-welded parts of the rings. Neither the industrially formed welds of single rings, nor the experimentally produced welds of contact areas were of mechanical strength inferior to the wire material. This is believed to be based on the transformation from alpha to alpha + beta structure due to the welding.

Besides that, the rings seem to gain in length and deform in such an extent without easily breaking. The contact area welds, appear to maintain their geometry and concave oriented deformation occurs on the longitudinal directed parts of a ring. Lengthening of the specimen predominantly occurs on the traverse-orientated parts of the rings. This aspect indicates the elasticity of the material and the ability of the welded region to withstand great forces. Important to mention is that the non-welded RRM undertook the same deformation shape as the welded RRM. That indicates the similarity of the physical properties of the two groups and the ability of the RRM to be used as a medical device.

The findings from the research illustrate, that the RRM can be a medical device with the advantage to be produced in every hospital, just with using an Nd-YAG laser machine. Apart from that further study is recommended of the use of a microidentation device (Diez-Perez et al. 2010) to take from different bone, mechanical properties values and try to examine the idea of using the same RRM but with different welding techniques or alloys of the same material with the aim to produce a stiffer or a ductile medical device that could be probably used on the different bone areas.

Conclusion

The experimental project demonstrates the possibility of the RRM to be used as a medical device for surgical applications. This is confirmed by the results of the axial tensile test, which give mechanical properties of the laser-welded specimens competent against the non-welded specimens. On the other hand, it should be noticed that in the project have been limitations, such as the welding process was done by an operator and not from a robot machine, where that could have as consequence some even better results. In addition, a further study of bending test should be performed using the same laser parameters and welding method in order to establish the ability of the medical device not only in axial tensile test but also in bending test. It could be important for further study the x-ray crystallography of the welded area to confirm any changes in the metallographic structure of the welded region.

Reference list

Billotte WG: Ceramic Biomaterials. In: The Biomedical Engineering Handbook Volume I, 2nd edition; ed. Borzino JD; CRC Press LLC, Springer, IEEE Press, Boca Raton 2000, 1-33

Brunski JB: Metals. In: Biomaterials science- An introduction to Materials in Medicine, 2nd edition; ed. Ratner BD, Hoffman AS, Schoen FJ, Lemons JE; Elsevier Academic Press, Amsterdam 2004, 137-153

Costantino PD, Tadros M, Wolpoe M: Principles of Facial Plating Systems. In: Facial Plastic and Reconstructive Surgery. 3rd edition; ed. Papel ID, Frodel JL, Holt GR, Larrabee WF, Nachlas NE, Park SS, Sykes JM, Toriumi DM; Thieme, New York 2009, 929-944

Cooper SL, Visser SA, Hergenrother RW, Lamba NMK: Polymers. In: Biomaterials science- An introduction to Materials in Medicine, 2nd edition; ed. Ratner BD, Hoffman AS, Schoen FJ, Lemons JE; Elsevier Academic Press, Amsterdam 2004, 67-79

Davis JR: Tensile testing. 2nd edition; ASM International, Cleveland 2004

Dawes C: Laser welding - A practical guide. (CB1 6AH), 1st edition; Abington Publishing, Woodhead Publishing, Cambridge 1992

Diez-Perez A, Güerri R, Nogues X, Cáceres E, Peña MJ, Mellibovsky L, Randall C, Bridges D, Weaver JC, Proctor A et al. (2010): Microindentation for In Vivo Measurement of Bone Tissue Mechanical Properties in Humans. Journal for Bone and Mineral Research 25(8), 1877–1885

Disegi JA, Kenned RL, Pilliar R: Overview. In: Cobalt-Base Alloys for Biomedical Applications, (STP1365); ed. Disegi JA, Kenned RL, Pilliar R; American Society for Testing and Materials, West Conshohocken 1999, vii-viii

Donachie MJ: Titanium A Technical Guide. 2nd edition; ASM International, Cleveland 2000

Hecht J, Teresi D: Laser Light of a million uses. Dover Publications Inc., New York 1998

IBM Corp. Released 2012. IBM SPSS Statistics for Windows, Version 21.0. Armonk, NY: IBM Corp.

Kumar C, Patel N (2013): Materials science. Encyclopedia Britannica online. Retrieved Web: 4 December 2013: http://www.britannica.com/EBchecked/topic/369081/materials-science/32301/General-requirements-of-biomaterials

Lazaridis N, Makos C, Iordanidis S, Zouloumis L (1998): The use of titanium mesh sheet in the fronto-zygomatico-orbital region. Case reports. Aust Dent J 43(4), 223-228

Leung PC: General Perspectives on Fracture Management. In: Current practice of fracture treatment: new concepts and common problems; ed. Leung PC; Springer-Verlag, Berlin 1994, 1-58

Lesić AR, Zagorac S, Bumbasirević V, Bumbasirević MZ (2012): The development of internal fixation - historical overview. Acta Chir Iugosl 59(3), 9-13

Materials Information Service: The Selection and Use of Titanium: A Design Guide, Vol. 641. (Issue 641); Institute of Materials, London 1995

NDT Resource Centre: (2012) Tensile properties. Retrieved September 17, 2012 from: URL:http://www.ndt-ed.org/EducationResources/CommunityCollege/Materials/Mechanical/Tensile.htm

Park JB: Biomaterials Introduction. In: The Biomedical Engineering Handbook Volume I. 2nd edition; ed. Borzino JD; CRC Press LLC, Springer, IEEE Press, Boca Raton 2000, 1-6

Townes CH: How the Laser Happened: adventures of a scientist. Oxford University Press, New York 1999

Van Veelen-Vincent MLC, Mathijssen I, Arnaud E, Renier D: Non-syndromic Craniosynostosis. In: European Manual of Medicine: Neurosurgery; ed. Lumenta CB, Di Rocco C, Haase J, Mooij JJA; Springer, Berlin 2010, 501-517

Welsch G, Boyer R, Collings EW: Materials Properties Handbook: Titanium Alloys. 4th edition; ASM International, Cleveland 2007

Williams DF: Definitions in biomaterials: Proceedings of a consensus conference of the European society for biomaterials, Chester, England, 3-5 March 1986, Vol. 4; Elsevier, New York 1987

WizCom Technologies Ltd (2007). Titanium. Retrieved September 04, 2013 from URL: http://www.answers.com/topic/titanium

Wolf N: Deep Penetration Welding – Heat Conduction Welding. In: Tailored Light 2 – Laser Application Technology, RWTH Aachen University Edition; ed. Poprawe R; Springer, Heidelberg 2011, 265-275

Annex

1. Universal Test Maschine Zwick 1446 with Software testXpert Version 12.1

General data

Force transducer: 10KN

Position sensor: Traverse

Specimen holder: Artikel-Nr. 8121 500N

Test area: Bottom (Tension space)

Top soft stopper at 800mm

Bottom soft stopper at 265mm

Recommended force limits: ±950N

No tolerance limits

Pre-load settings

Pre-load: 2MPa

Pre-load speed: 10mm/min

Pre-load time reached: 60s

Kept pre-load time: 5s

Force zeros after pre-load reached

Young’s modulus settings

Established through the tangent in the graph

Start at 50 MPa

Tensile test data

Test-speed: 60mm/min

Power-operated shut-down at 80% Fmax (Tensile strength)

After test settings

Specimen released

Speed of release: 10mm/min

2. Hooke‘s Law of elasticity

Definition

“The force F applied to a spring is directly proportional to the spring’s extension or compression, x, provided the elastic limit is not exceeded.” k = constant = Young’s modulus

F=-kx

3. Statistical analysis

The ROOT Data Analysis Framework was used for the statistical analysis.

The data are fit by a first order polynomial function $E = a + bI$ using a linear regression approach for modeling the experimental data. The fit method provides the errors Δα and Δb

One way in which a measure of goodness of fit statistic can be constructed, in the case where the variance of the measurement error is known, is to construct a weighted sum of squared errors:

$$\chi^2 = \sum \frac{(O - E)^2}{\sigma^2}$$

where χ2 is the known variance of the observation, O is the observed data and E is the theoretical data.

The errors Δα and Δb are used to calculate the errors on the energy at a given Current (I) with the propagation of errors, as follows:

$$\Delta E = \sqrt{\left(\frac{\partial E}{\partial a}\right)^2 \Delta a^2 + \left(\frac{\partial E}{\partial b}\right)^2 \Delta b^2} = \sqrt{\Delta a^2 + I^2 \Delta b^2}$$

Patent of the university medical hospital Göttingen

(19) Bundesrepublik Deutschland
Deutsches Patent- und Markenamt

(10) **DE 10 2006 055 432 A1** 2008.05.29

(12) **Offenlegungsschrift**

(21) Aktenzeichen: **10 2006 055 432.9**
(22) Anmeldetag: **22.11.2006**
(43) Offenlegungstag: **29.05.2008**

(51) Int Cl.[8]: ***B21F 27/00*** (2006.01)
F41H 1/02 (2006.01)

(71) Anmelder:
Georg-August-Universität Göttingen Stiftung Öffentlichen Rechts (Bereich Humanmedizin), 37075 Göttingen, DE

(74) Vertreter:
Gramm, Lins & Partner GbR, 30173 Hannover

(72) Erfinder:
Buchhorn, Gottfried Hans, 37077 Göttingen, DE; Wellnitz, Jörg, Prof. Dr.-Ing., 85137 Walting, DE; Schultz, Wolfgang, Prof. Dr. med., 37085 Göttingen, DE

(56) Für die Beurteilung der Patentfähigkeit in Betracht gezogene Druckschriften:
DE 102 19 853 A1
DE 37 02 916 A1
DE 5 90 431 A
DE 5 13 822 A
JP 20044347294 A;

Die folgenden Angaben sind den vom Anmelder eingereichten Unterlagen entnommen

Prüfungsantrag gemäß § 44 PatG ist gestellt.

(54) Bezeichnung: **Bauteil aus Geflechtelementen**

(57) Zusammenfassung: Die Erfindung betrifft ein Bauteil mit einem Geflecht aus mehreren, ineinander greifenden, geschlossenen Geflechtelementen. Gemäß einem zweiten Aspekt betrifft die Erfindung ein Verfahren zum Herstellen eines Bauteils. Aufgabe der Erfindung ist es, Nachteile im Stand der Technik zu überwinden. Diese Aufgabe wird dadurch gelöst, dass einzelne Geflechtelemente so verbunden sind, dass das Geflecht in mindestens einer Raumrichtung schubstabil ist.

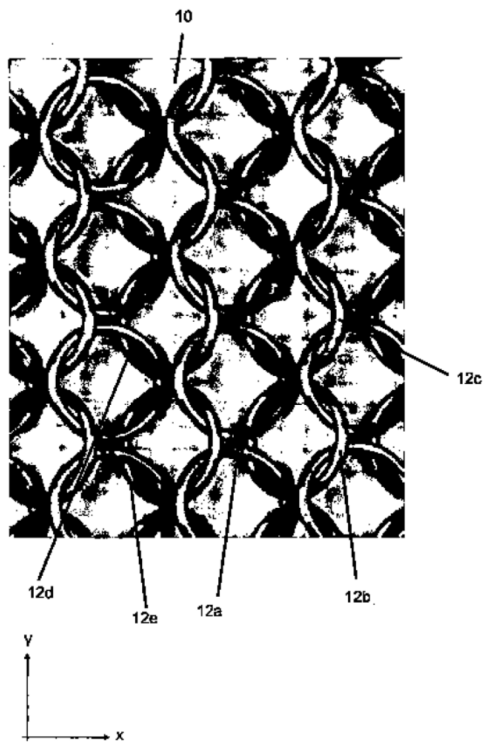

4. Normal Q-Q Plot Graphs

Control Group: Non-welded specimens
Experimental Group: Welded specimens

Plot 1

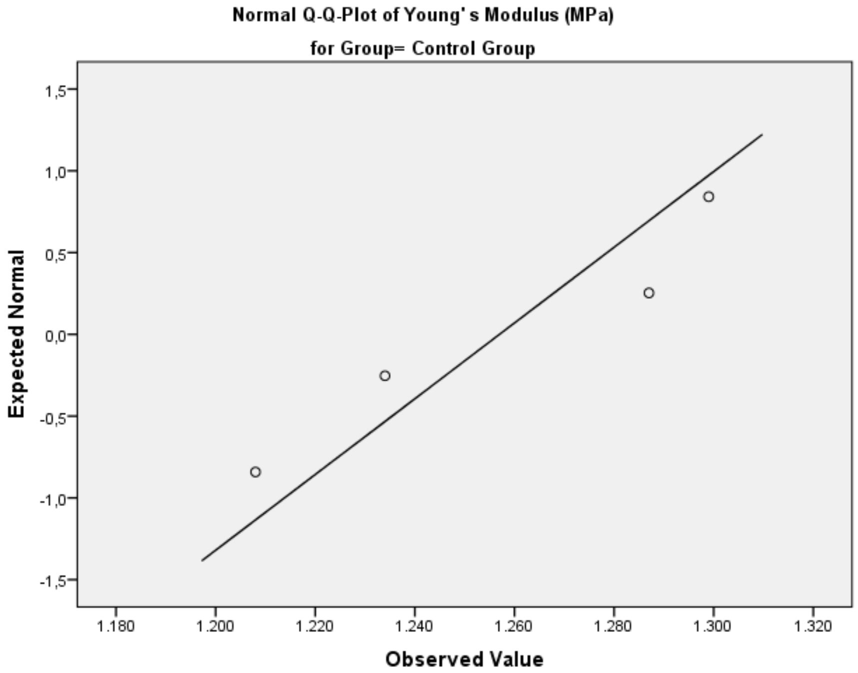

Plot 2

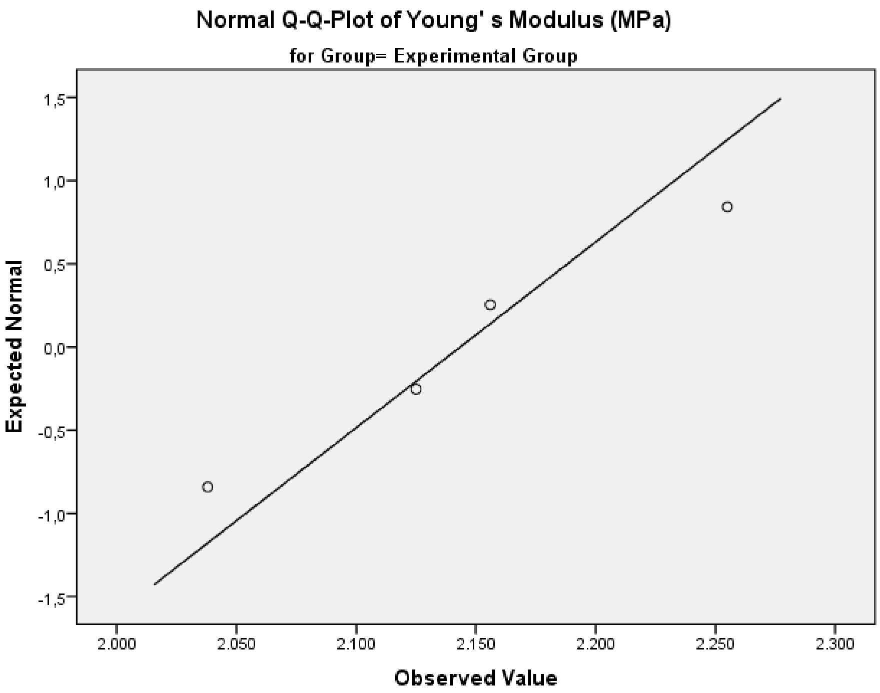

Plot 3

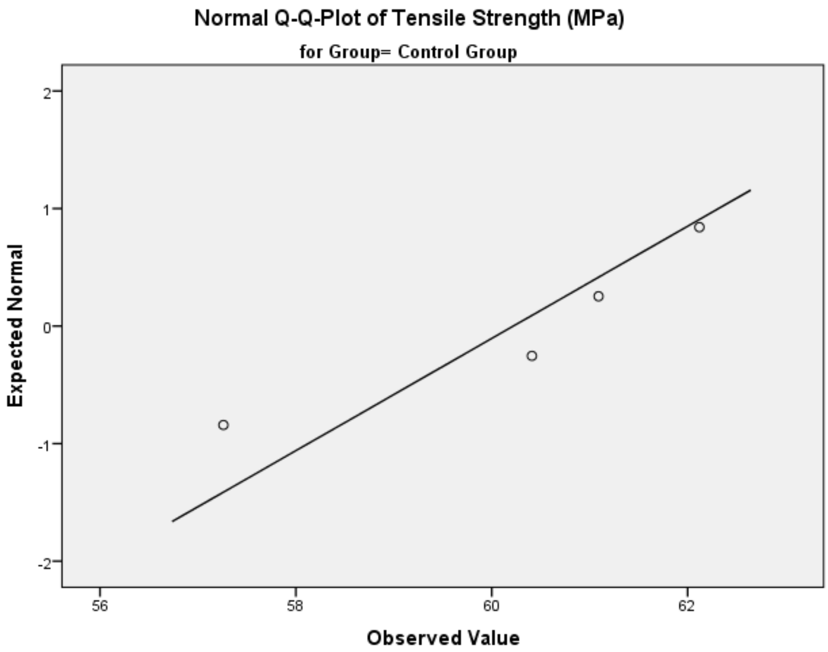
Normal Q-Q-Plot of Tensile Strength (MPa)
for Group= Control Group
Expected Normal
Observed Value
2
1
0
-1
-2
56
58
60
62

Plot 4

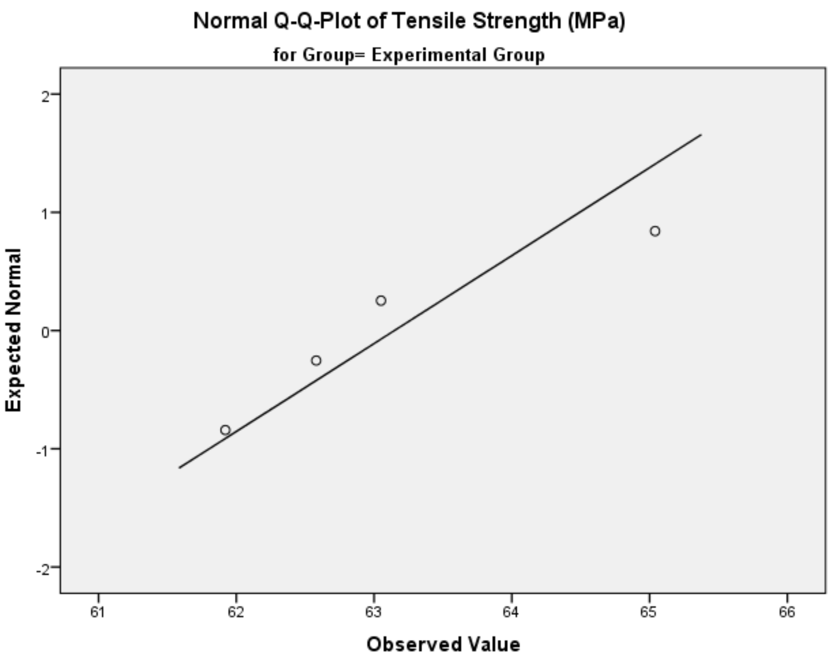
Normal Q-Q-Plot of Tensile Strength (MPa)
for Group= Experimental Group
Expected Normal
Observed Value
2
1
0
-1
-2
61
62
63
64
65
66

Plot 5

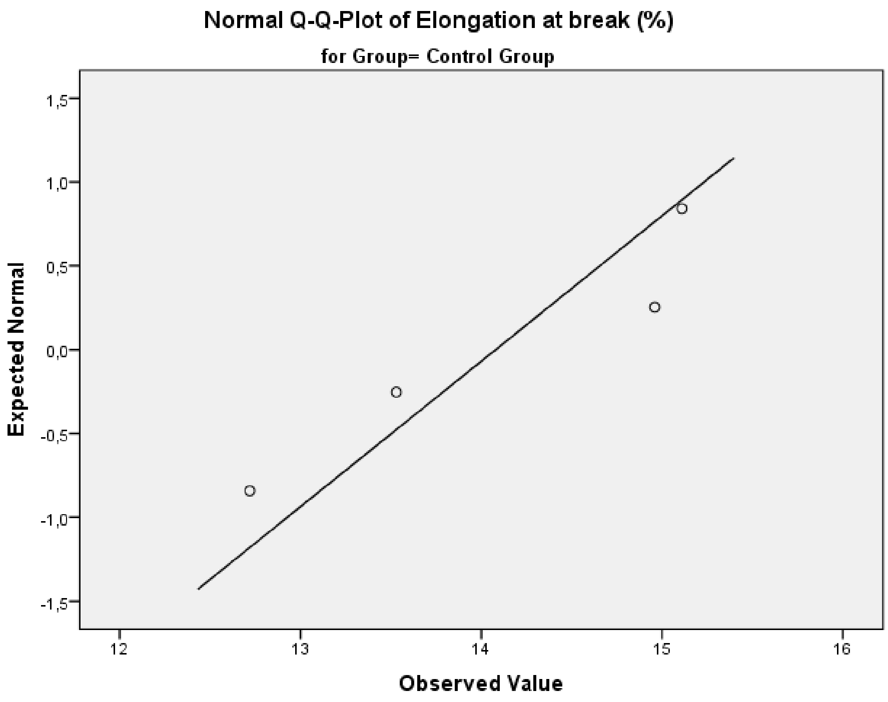
Normal Q-Q-Plot of Elongation at break (%)
for Group= Control Group
Expected Normal
1,5
1,0
0,5
0,0
-0,5
-1,0
-1,5
12
13
14
15
16
Observed Value

Plot 6

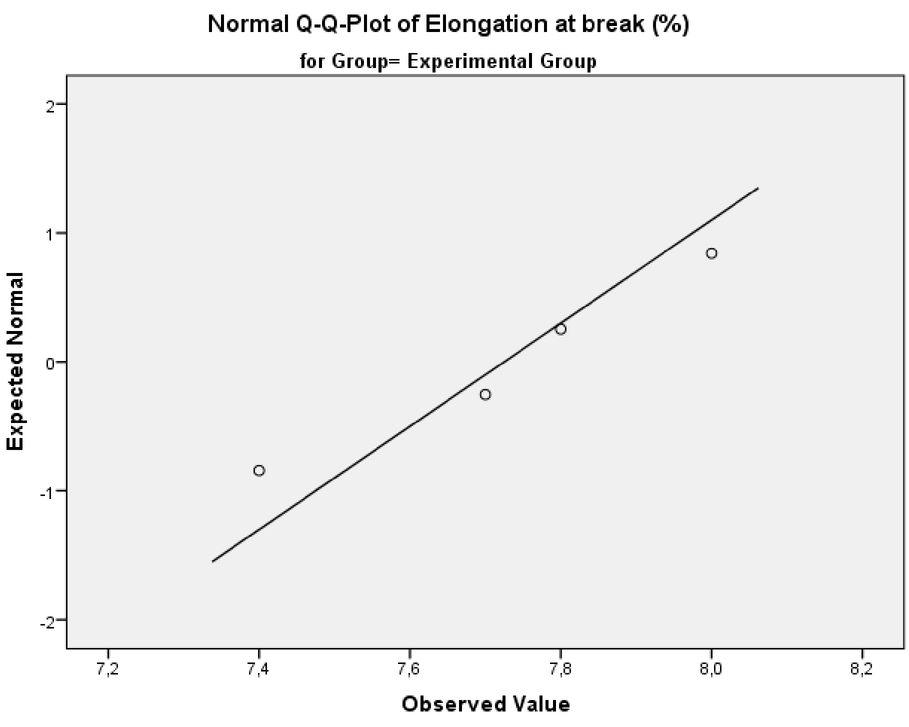
Normal Q-Q-Plot of Elongation at break (%)
for Group= Experimental Group
Expected Normal
2
1
0
-1
-2
7,2
7,4
7,6
7,8
8,0
8,2
Observed Value

Plot 7

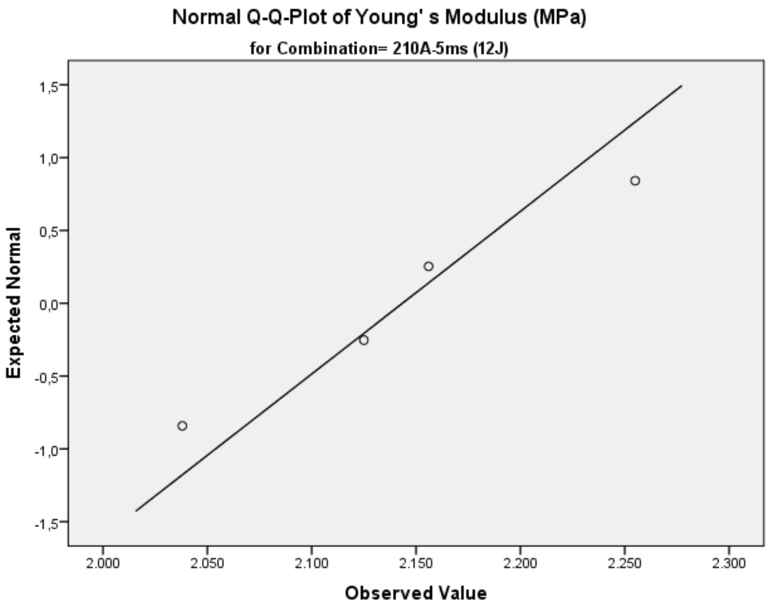
Normal Q-Q-Plot of Young' s Modulus (MPa)
for Combination= 210A-5ms (12J)
Expected Normal
Observed Value
1,5
1,0
0,5
0,0
-0,5
-1,0
-1,5
2.000
2.050
2.100
2.150
2.200
2.250
2.300

Plot 8

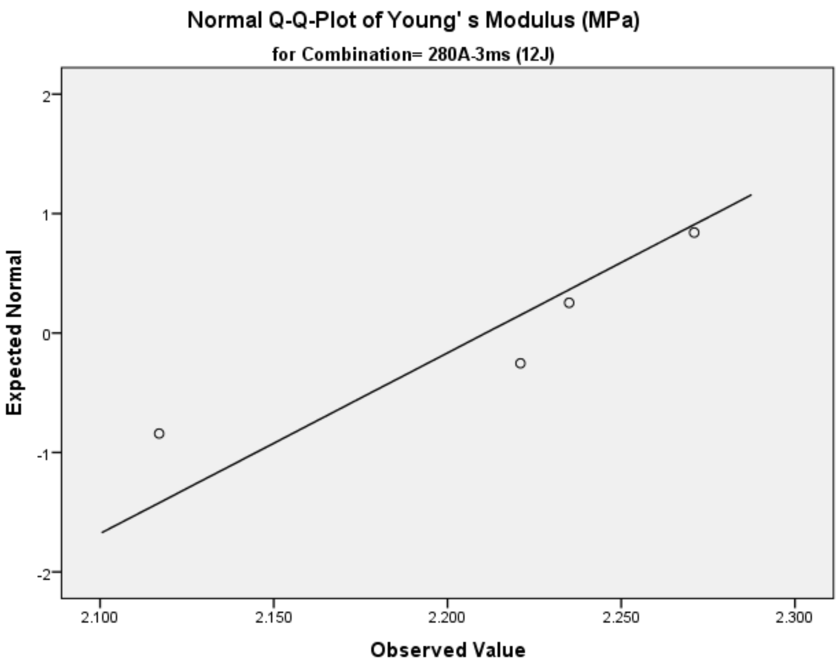
Normal Q-Q-Plot of Young' s Modulus (MPa)
for Combination= 280A-3ms (12J)
Expected Normal
Observed Value
2
1
0
-1
-2
2.100
2.150
2.200
2.250
2.300

Plot 9

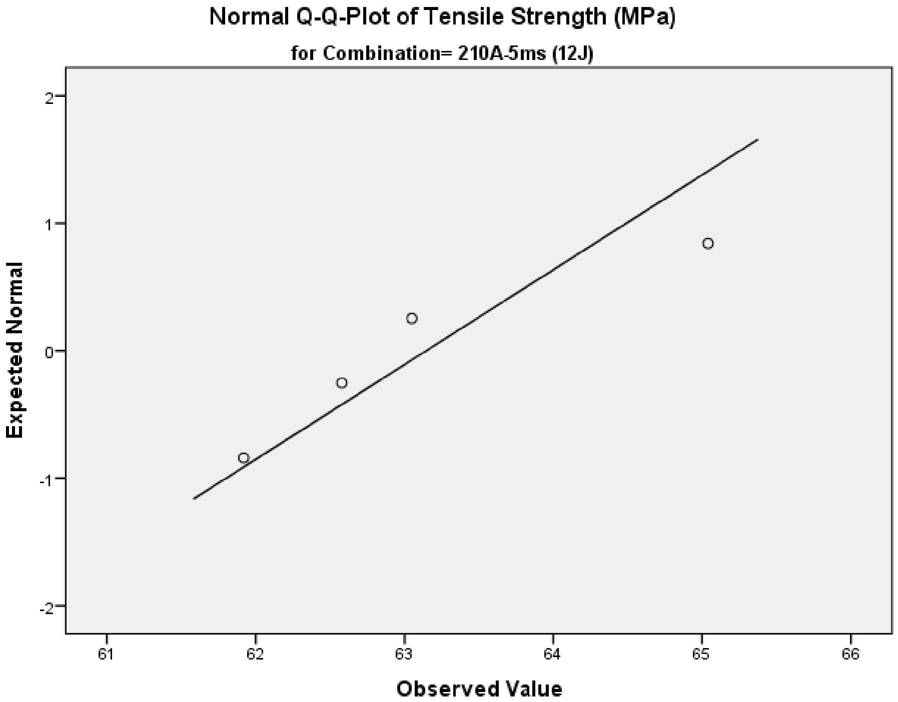

Plot 10

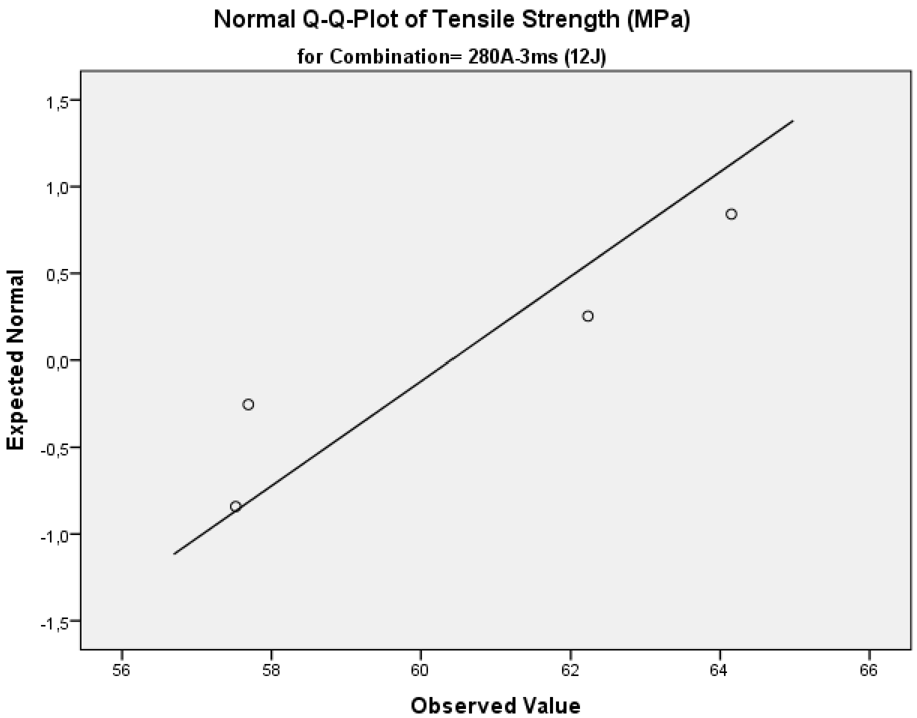

Plot 11

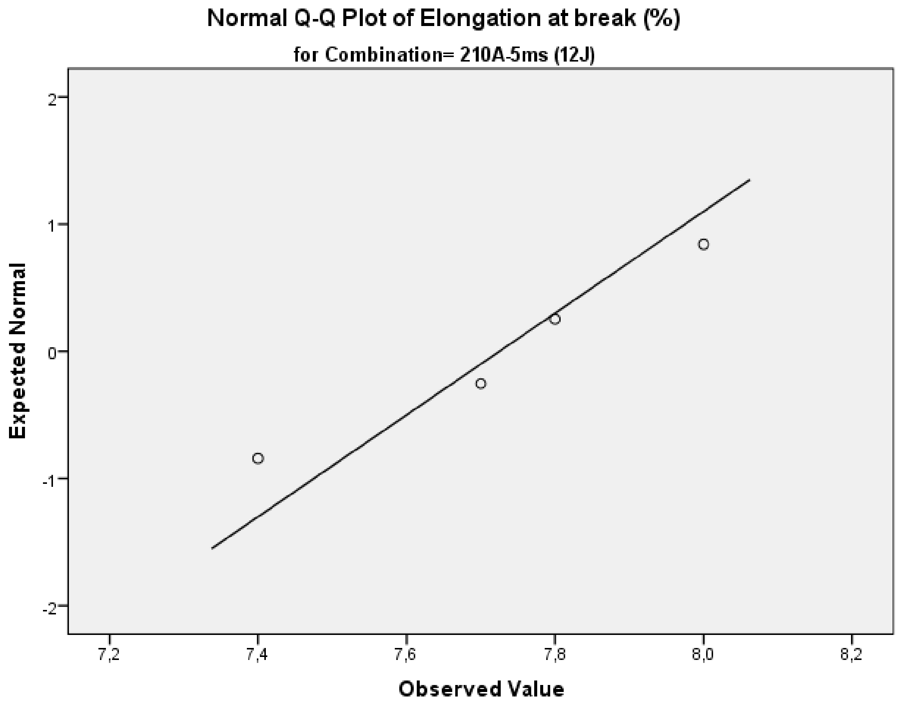

Plot 12

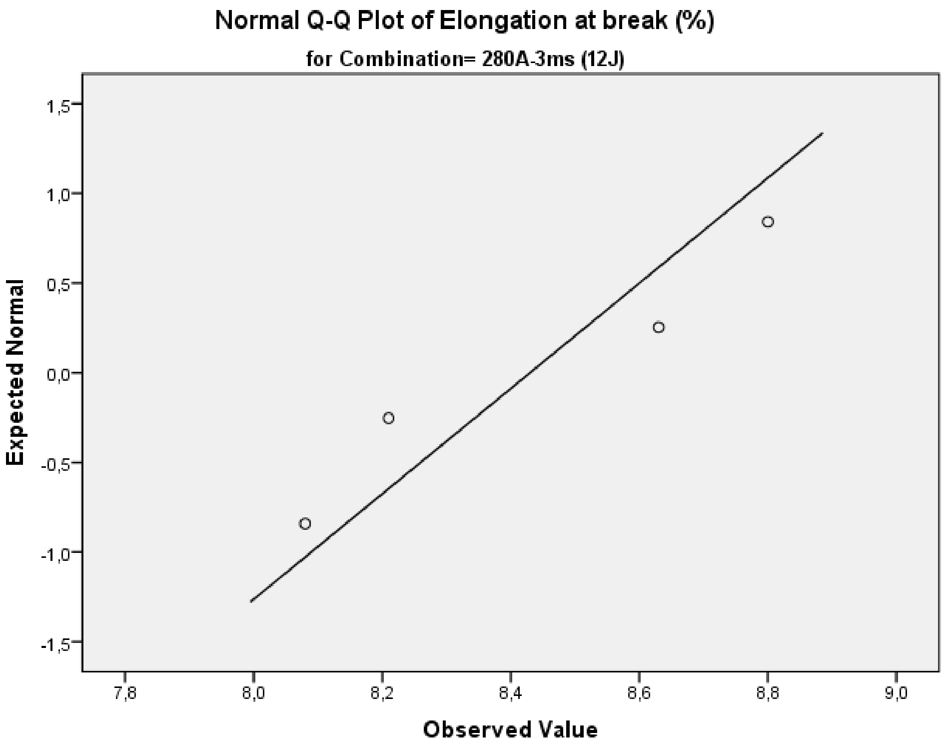

Plot 13

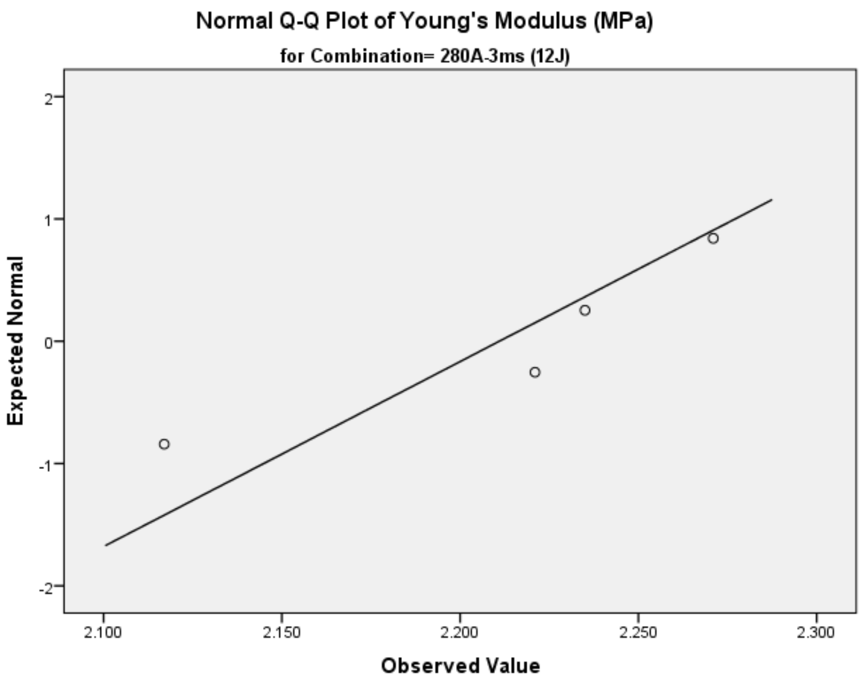

Plot 14

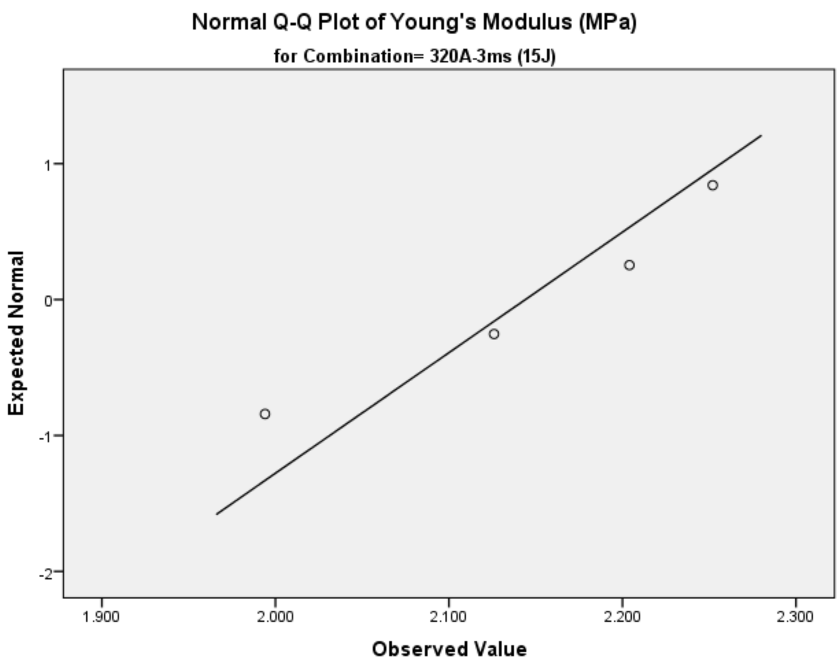

Plot 15

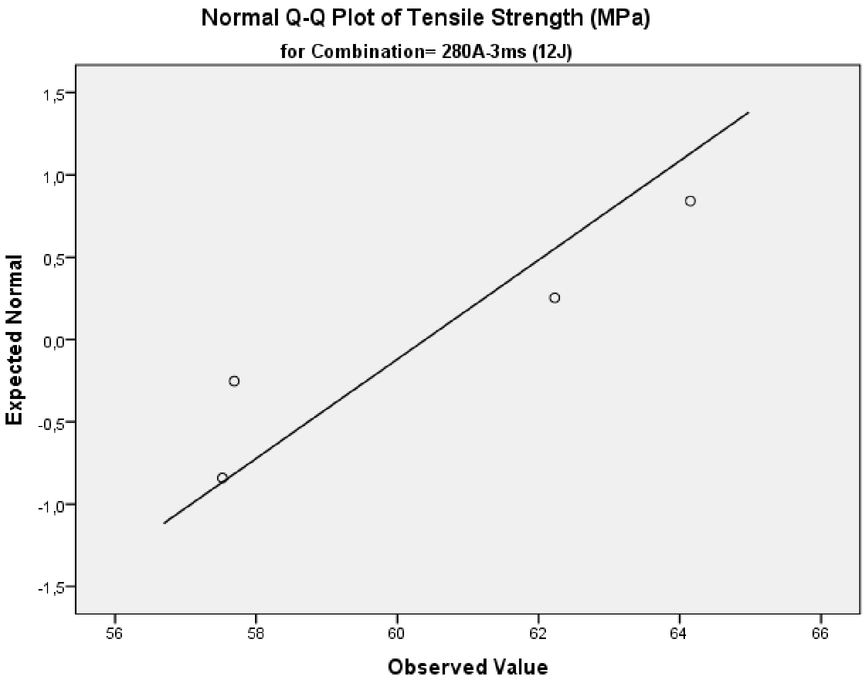

Plot 16

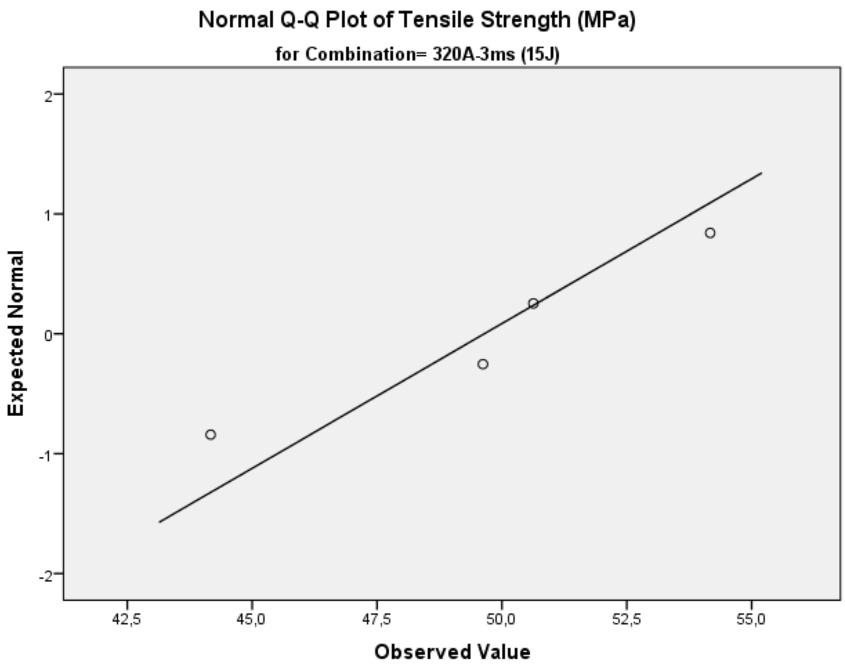

Plot 17

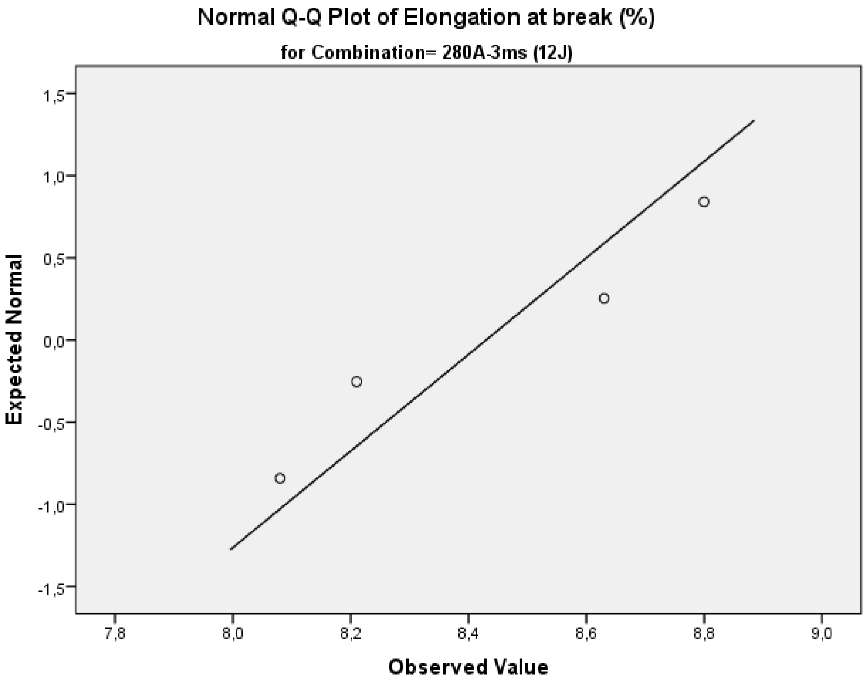

Plot 18

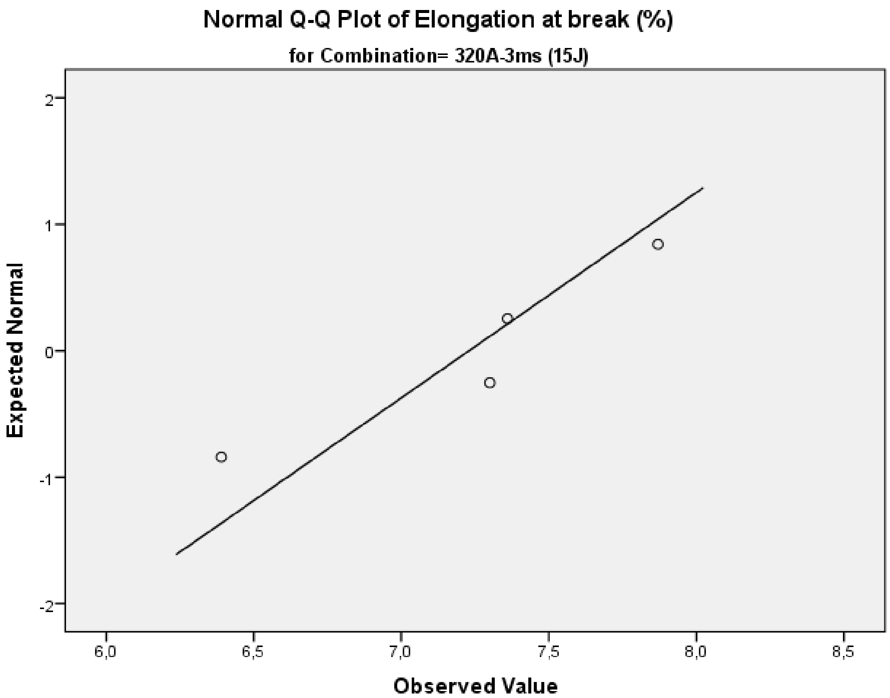

Acknowledgments

Prof. Dr. W. Schultz, Orthopaedic Department, University Hospital Göttingen for the definition of the project and continuous support
Prof. Dr. N. Gersdorff for the allowance and support using the universal testing machine as well as Mr. J. Riechel and colleagues for support, Department for Dental Prosthetics, University Hospital Göttingen
Prof. Dr. D. Stalke and Mr. Ch. Maaß, Institute for Anorganic Chemistry University Göttigen for advice and laboratory support regarding the alpha case of titanium
Dr. J. Ihlemann, Laserzentrum Göttigen and Mr. U. Turek, Tanaka GmbH for energy measurements of the laser application
Mr. C. Lott, Mr. Th. Kerl and team, Mechanical Works for Research and Development, University Hospital Göttingen for the manufacture of the supplementary equipment
Dr. Zinonas Zinonos PhD Research Fellow, II. Physikalisches Institut,
Georg-August-Universität Göttingen
Anastasia Kanari M.A, for advice in Statistical analysis of the project
Mrs Constantinou Chrystalla, English teacher in Pascal English School for the revision of the English language